THE UNIVERSITY OF ADELAIDE

SCHOOL OF ELECTRICALAND ELECTRONIC ENGINEERING
ADELAIDE, SOUTH AUSTRALIA 5005

ELEC ENG 3019 Practical Electrical and Electronic Design III

High Frequency Oscillator Formal Report

Lecturer: **Mr. Andrew Allison**
Laboratory Instructors: **Dr. Peter Cooke**
Mr Refaat Gregory

Student: **Zhiyang Ong** ▮▮▮▮

Declaration

The author, Zhiyang Ong ████████████████████, declare the following to be of his own work, unless otherwise referenced, as defined by The University of Adelaide's policy on plagiarism.

Abstract

The design of the Colpitts oscillator to operate at 20.0 MHz is described, and its simulation results are discussed. Also, the different sources of signals that can be measured are described and discussed. In addition, the loading effect on the oscillator, and its input drive is described. Moreover, different points in the circuit have different levels .of signal purity and signal integrity. Lastly, conclusions from the experiment are discussed.

Table of Contents

1.   Introduction

1.1   Objectives (Sarkies, K, Cooke, P & Allison, A 2003)

The objectives for the high frequency oscillator practical are to:

1. Design the oscillator to perform at the specified frequency that is accurate over a range of component variations.
2. Determine the effects of circuit layout and movements on oscillation behaviour.
3. Measure and evaluate the distortion of the oscillator waveform using spectral techniques.

1.2   Background Information

The radio spectrum comprises of a variety of signals at various amplitudes and frequencies. Each signal is superimposed onto a high frequency carrier signal to transmit information for audio or video broadcast over long distances so that other transmissions can take place in the radio spectrum (Sarkies, K, Cooke, P & Allison, A 2003).

Oscillators are used by radio transmitters to establish the frequency of transmission. The frequency of oscillation has to be stable to avoid interference with other transmissions at adjacent frequencies so that receivers can "lock onto" the transmissions (Sarkies, K, Cooke, P & Allison, A 2003).

In a super-heterodyne radio receiver, the oscillator plays a complementary role. The receiver separates unwanted signals from the desired signal to produce a clean base band output with minimal noise of interference as part of audio or video broadcast. As illustrated in Figure 1, this process is carried out in stages. The Radio Frequency (RF) filter, which is the first stage of the process, filters out unwanted signals that are not adjacent to the desired frequency. The mixer multiplies the output of the oscillator with the filtered signal from the RF filter to much lower intermediate frequencies (IF) for more precise IF filters are used to separate the desired frequency from the remaining unwanted frequencies (Sarkies, K, Cooke, P & Allison, A 2003).
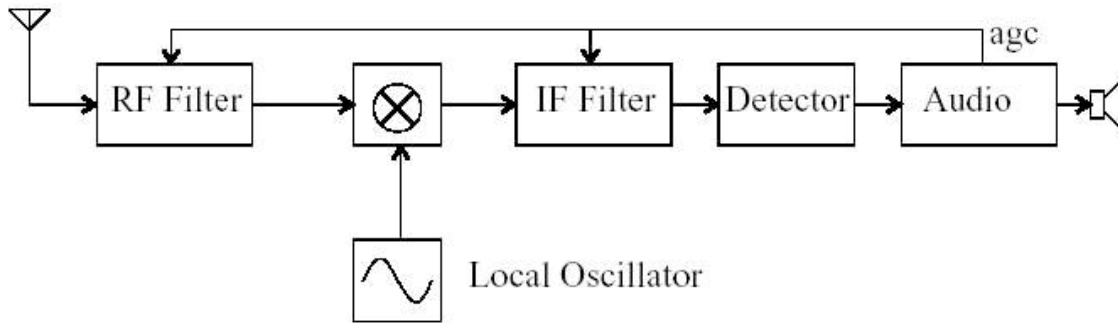
Figure 1. Super-heterodyne Radio Architecture (Sarkies, K, Cooke, P & Allison, A 2003)

Oscillators use the concept of positive feedback to enhance instability. The output of the active device, such as a Bipolar Transistor, is feed back into the input. This leads to a rapid build up in the amplitude of the output. By arranging the circuit to disconnect the source of energy when the maximum amplitude at the output is reached, the output will fall to zero when the energy source is disconnected. This process is repeated to provide a steady periodic signal of waveform depending on the mechanism used (Sydenham, PH 1983).
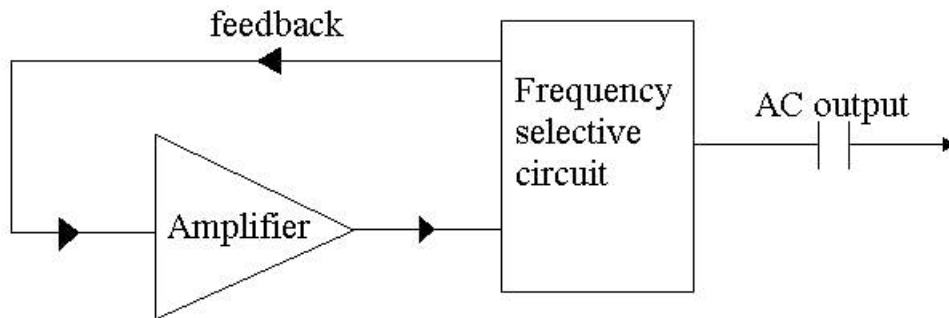
Figure 2. Basic block diagram of a feedback oscillator (Adapted from Sydenham, PH 1983).

As shown in Figure 2, a wave-shaping circuit that determines the time behaviour of the positive feedback is fed with in-phase signals from an amplifier to produce oscillations. Hence, for a high open-loop gain of the oscillator circuit, only a small amount of in-phase signal is required to produce oscillations. For the feedback circuit to oscillate at a desired frequency, the following three criteria must be satisfied by choosing suitable component values. Firstly, there should be no phase shift between the amplifier and the frequency selective circuit, as illustrated in Figure 2, at the desired frequency so that instability exists to provide oscillations. Secondly, the voltage gain of both the amplifier and the frequency selective circuit must be greater than unity at the desired

frequency. Lastly, the voltage gain must drop to unity once oscillations begin to prevent the amplitude of the output from increasing exponentially (Sydenham, PH 1983).

The last two points are considered in detail as follows. For the oscillator to oscillate at the desired frequency, a non-linear circuit is required to provide gain control for $A * \beta > 1$, where A is the open-loop gain of the amplifier and β is the gain of the frequency selective circuit. This is the required condition to increase the amplitude of the oscillator. Note that, if $A * \beta < 1$, the oscillator will not oscillate. Set $A * \beta$ to be slightly greater than unity to ensure the start of oscillation. When the desired amplitude of the oscillator's output is reached, the non-linear frequency selective circuit comes into action and reduces the loop gain, $A * \beta$, to unity to sustain the oscillation at the desired frequency. Should the loop gain fall below unity, the frequency selective circuit increases it back to unity (Sedra, AS & Smith, KC 1998).

1.3   Scope and limitations of this study

The scope of this experiment is to design and build an oscillator to perform at the specified frequency, which is at 20 MHz. Hence, oscillators that work at other high frequencies, which are in the 3 MHz to 30 MHz range, are not considered. Very high frequencies, which are frequencies ranging from 30 MHz to 300 MHz, and beyond are not examined (*SearchNetworking.com* [Online] 2003).

The restricted access to measuring instruments and circuit-building equipment as well as the lack of ample time to be spent for this experiment prevents the coverage of all related Electrical and Electronic Engineering concepts, such as the Stability Criterion of an oscillator, the Barkhausen Criterion for feedback oscillators (Millman, J & Halkias, CC 1967) and the Nyquist criterion for determining stability in feedback circuit (Schwarz SE & Oldham, WG 1993). Hence, only the concepts of DC biasing, small-signal AC analysis, feedback, gain, resonance in electronic circuits, squegging oscillators, purity of signals and buffer amplifiers are considered in this practical.

1.4   Method of approach

A Colpitts oscillator, using a Bipolar Junction Transistor (BJT) in a common emitter amplifier configuration, is designed and constructed to work at the specified frequency that is accurate over a range of component variations. Changes of the circuit's components will be made to determine how the behaviour at the output of the oscillator is affected. The Fast Fourier Transform spectral technique is used to indicate the amount of distortion present in the oscillator's output waveform.

Finally, results of the experiment are discussed and knowledge of the high frequency oscillator are expanded or clarified.

2. Design and construction of the oscillator

2.1 Design of the oscillator

2.1.1 Selection of an oscillator circuit

Several circuits that function as oscillators include the Armstrong oscillator, Hartley oscillator, Quartz Crystal oscillator, phase shift oscillator and the Wien-bridge oscillator (Sydenham, PH 1983); other electronic circuits that oscillate are LC- or active filter tuned oscillators as well as the quadrature oscillator (Sedra, AS & Smith, KC 1998). The Colpitts oscillator was recommended for this oscillator design in the instruction handout for this experiment (Sarkies, K, Cooke, P & Allison, A 2003).

The Colpitts oscillator is formed around a resonant (tuned) circuit, which allows the output frequency of the oscillator to be specified, with a pair of capacitors, C_1 and C_2. One side of the tuned circuit provides a positive feedback to the input of the amplifying circuit whilst the other side drives the amplifying circuit. By manoeuvring the amplifying and resonant circuits around, different configurations of the Colpitts oscillator can be obtained in practice (Sarkies, K, Cooke, P & Allison, A 2003).

As shown in Figure 3, the resonant circuit of the suggested Colpitts oscillator design consists of an inductor L and two capacitors, C_2 and C_2. The BJT forms the amplifying element of this Colpitts oscillator. The resistors R_1, R_2 and R_E are used to bias this BJT. The capacitor C_{B1} is used as a bypass capacitor to ensure that the nodes marked as Test Points (TP) one (TP_1) and two (TP_2) are effectively the same node at high frequencies. C_{B2} is also a bypass capacitor that grounds the BJT's emitter to earth at high frequencies to prevent negative feedback from reducing the gain of the oscillator's amplifying circuit. L_{B1} is used as a bypass inductor to allow TP_1 to oscillate freely at high frequencies. If L_{B1} is not used in this oscillator circuit, desired high-frequency signals will be shorted out through the DC power supply (Sarkies, K, Cooke, P & Allison, A 2003).
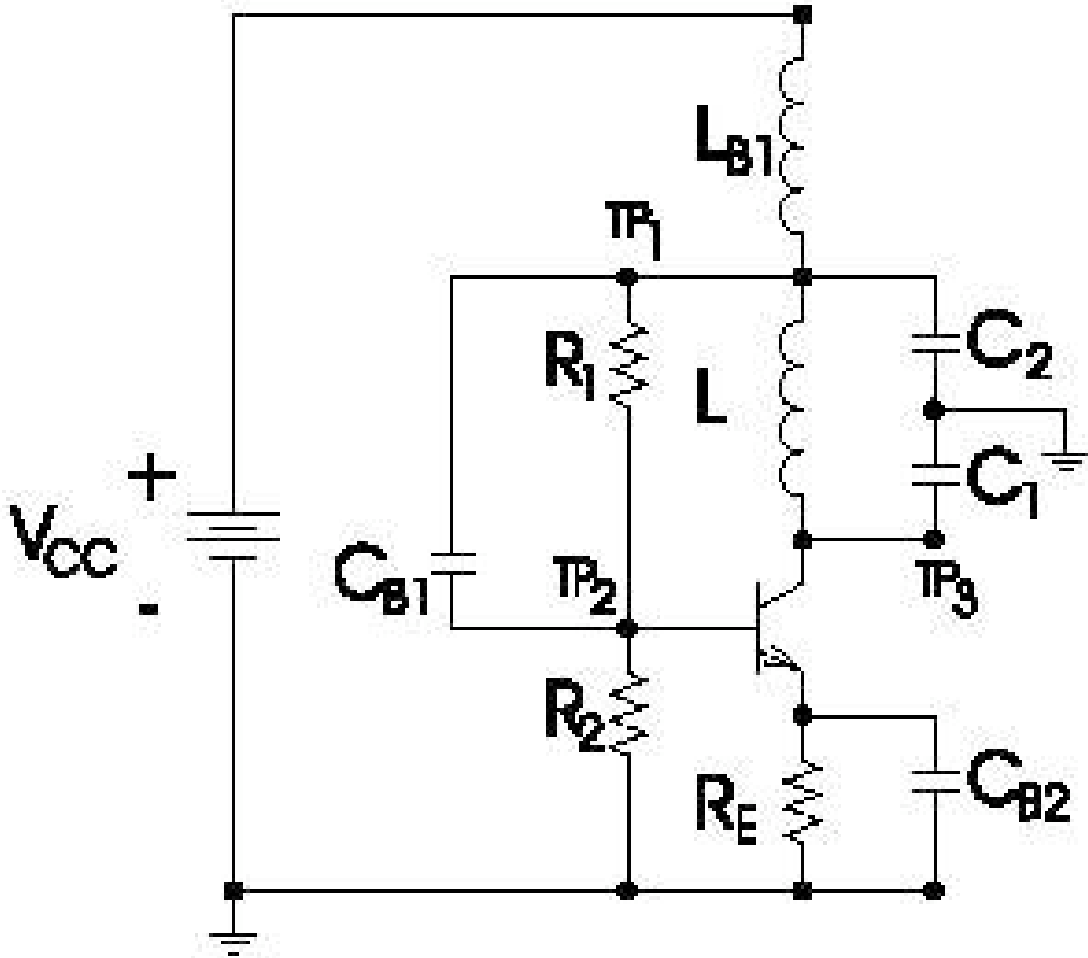
Figure 3. A schematic circuit diagram for the Colpitts Oscillator (Sarkies, K, Cooke, P & Allison, A 2003).

2.1.2   Specifications (Sarkies, K, Cooke, P & Allison, A 2003)

1. Supply voltage: V_{CC} = 10 V

2. Output frequency: $f_o = \omega_o / (2\pi)$ = 20 MHz, with accuracy of ±1%.

3. Output voltage to earth from TP$_3$: $V_2 \geq 1.0$ V (peak amplitude)

4. All post-mentioned constraints, found in Sections 2.1.3 and 2.1.5, must be satisfied.

5. Start your design using a BC549 NPN BJT as well as L = 1μH.

2.1.3 DC Bias Constraints (Sarkies, K, Cooke, P & Allison, A 2003)

1. A large transconductance g_m is desired so that a large gain for the common emitter amplifier can be obtained.

2. $V_{CE} = \frac{1}{2}V_{CC}$, designers' choice.

3. Assume the base-emitter voltage is almost constant,

$$V_{BE} = (V_B - V_E) \approx 0.6 \text{ V}$$

4. Acceptable power dissipation in R_E: $(V_E)^2 / R_E \leq P_{max}$

5. Acceptable power dissipation in the BJT: $V_{CE} * I_C \leq P_{max}$

6. Acceptable power dissipation in R_1: $(V_{CC} - V_B)^2 / R_1 \leq P_{max}$

7. Acceptable power dissipation in R_1: $(V_B)^2 / R_2 \leq P_{max}$

8. A "large" chain current: $I_{ch} = V_{CC} / (R_1 + R_2) >> I_B$ so that the BJT is biased properly. Note that $I_B = I_C / \beta$

9. The forward current gain of the transistor is large, $\beta = h_{fe} \geq 100$ so $I_c \approx I_E$

10. Assume that no package will dissipate more than $P_{max} = 125$ mW (designers' choice)

2.1.4 DC Bias Analysis

A regulated laboratory DC power supply is used provide the supply voltage.

At very low frequencies, the bypass capacitors, C_{B1} and C_{B2}, present enormous amounts of impedance to current. Hence, they can be considered open circuits at DC. Conversely, the blocking inductor, L_{B1}, presents insignificant impedance to current at DC. Hence, L_{B1} is effectively a short circuit at DC. The DC equivalent circuit is shown in Figure 4 (Sarkies, K, Cooke, P & Allison, A 2003).
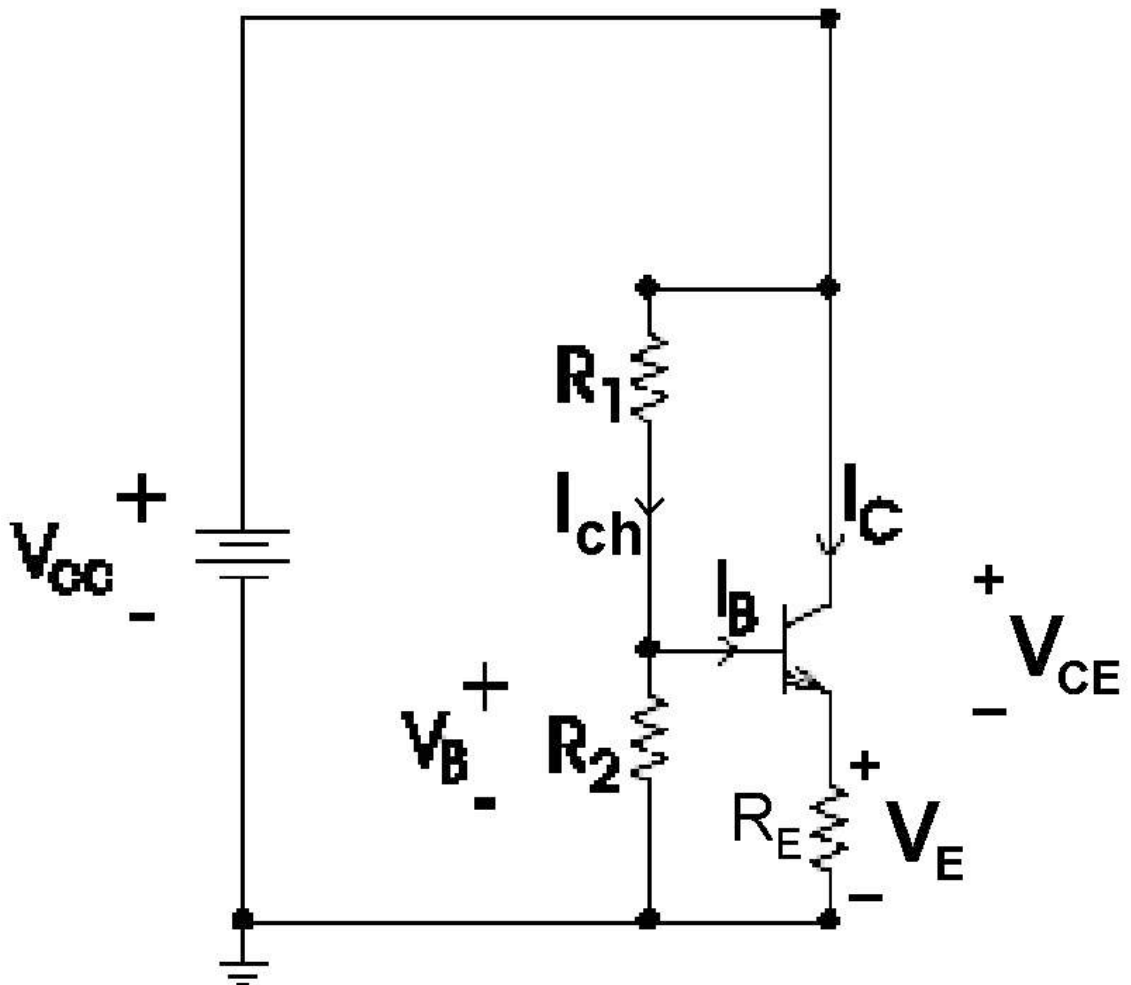
Figure 4. This is the very low frequency or "DC" equivalent circuit for the Colpitts Oscillator shown in Figure 3 (Adapted from Sarkies, K, Cooke, P & Allison, A 2003).

$V_{BE} = (V_B - V_E)$. Assume that $V_{BE} \approx 0.6$ V because V_{BE} does not change very much, according to Shockley's equation applied to the base-emitter P-N junction of the BJT, when i_c changes and a bigger current is drawn. Hence, V_{BE} is assumed constant (Allison, A 2003, pers. comm., 14 March).

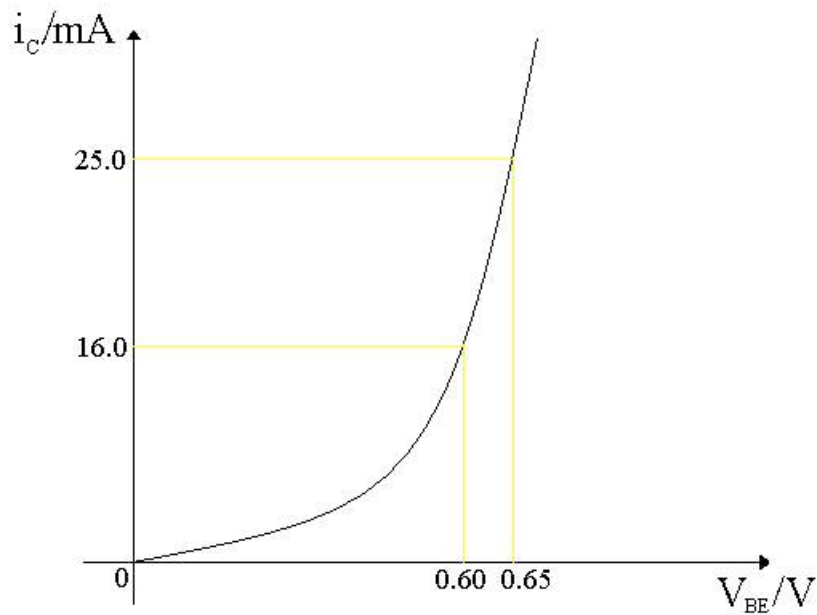Shockley's equation for the BJT: $i_c = i_s * exp(V_{BE} / (2 * V_T) - 1)$ (Allison, A 2003, pers. comm., 14 March).

Figure 5. This is the graph of i_c against V_{BE} for V_{CE} = 5 V (Adapted from Hambley, AR 2000)

As shown in Figure 5, the increase of i_c from 16 mA to 25 mA is much greater than the increase of V_{BE} from 0.60 V to 0.65 V. Thus, as aforementioned, V_{BE} changes very little for a big change in i_c.

Choose V_{CE} = ½V_{CC}, as suggested by Dr. Cooke. Dr. K. Saris suggested using V_{CE} = 0.9 V_{CC}. An investigation has yet to be conducted to determine which designers' choice is better (Allison, A 2003, pers. comm., 14 March).

The design of the Colpitts oscillator began with using the BC549 NPN Transistor as the BJT since there is a good supply of them in the laboratories of Adelaide University's Department of Electrical and Electronic Engineering, PSpice models for these BJTs are available and BC549 NPN BJTs have been successfully implemented in oscillator designs (Allison, A 2003, pers. comm., 14 March).
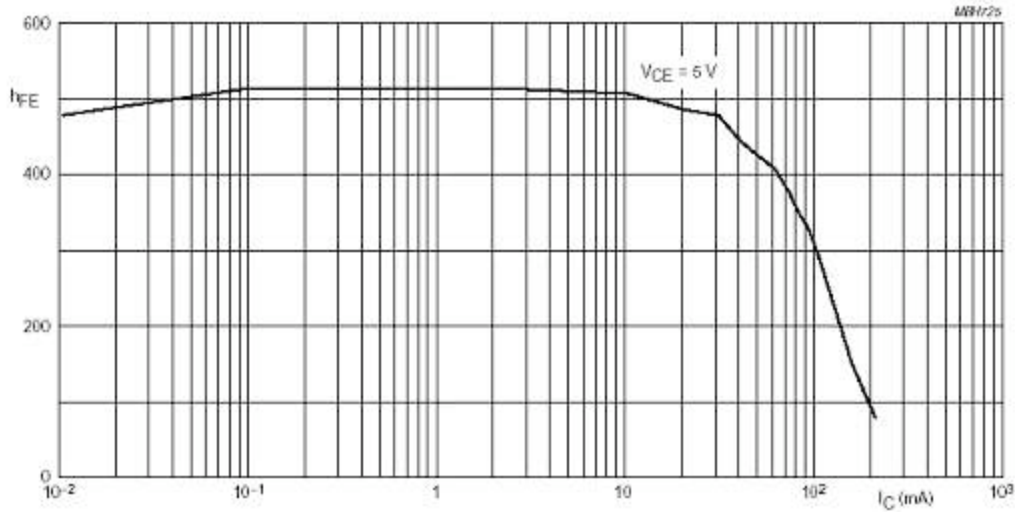
Figure 6. DC current gain; typical values (Philips Semiconductors 1999).

With reference to Figure 6, take the DC current gain, $\beta = h_{fe} = 500$ for 5 V V_{CE} (Philips Semiconductors 1999). Note that β will vary as the temperature changes.

For common emitter amplifiers, a big gain is desired. This implies that g_m must be big. This also implies that I_C must be large but not so large that the transistor exceeds the maximum power dissipation for the package, which is 500 mW (Philips Semiconductors 1999).

Choose $P_{max} = 80mW$ for a conservative design where the wires and electronic circuit components are not likely to be burned.

Since $V_{CE} = V_C - V_E$, and $V_{CE} = \frac{1}{2}V_{CC}$,

V_B can be calculated using $V_{BE} = V_B - V_E$

Let the current passing through R_1 and R_2 be the "chain" current, I_{ch}, where $I_{ch} = V_{CC}/(R_1 + R_2)$

Assume that $I_B = I_C/\beta$ is much smaller than I_{ch} so that the voltage divider principle can be applied to estimate V_B in terms of V_C and then work out the ratio of

$$(R_1/R_2) = (V_{CC}/V_B) - 1$$

By definition, $(A \gg B) \Leftrightarrow (A > 30 * B)$,

where the number "30" is a 3% safety factor (Sarkies, K, Cooke, P & Allison, A 2003). Hence, the equality relating I_{ch} and I_B, $I_{ch} \gg I_B$, becomes

$$V_{CC}/(R_1 + R_2) > 30 * I_C/\beta$$

From the DC bias calculations in Appendix A,

$I_C = 16$ mA,

$I_E = 16$ mA,

$I_B = 32$ μA,

$I_{ch} = 0.96$ mA,

$R_1 = 4.58$ kΩ,

$R_2 = 5.83$ kΩ,

$R_E = 312.5$ Ω,

2.1.5 Small-Signal AC Constraints (Sarkies, K, Cooke, P & Allison, A 2003)

1. The oscillator will oscillate if $g_m * R \gg C_2 / C_1$,

   where R is composed of r_π and R_2 in parallel, $1/R = 1/r_\pi + 1/R_2$. For large oscillations to occur, g_m must be very large. The amplitude of the signals is limited by the non-linear aspects of the BC549 NPN BJT. Hence, the loop gain is reduced to unity to sustain the oscillation (Sedra, AS & Smith, KC 1998).

   The Colpitts oscillator is a self-limiting oscillator that reduces the gain of the BJT til it is below its small-signal value as the amplitude of the oscillator increases. When the effective gain is reduced to a point where the Barkhausen criterion is satisfied, the corresponding amplitude of oscillation is maintained (Sedra, AS & Smith, KC 1998).

2. The oscillator will operate at the right frequency $\omega_0 = 2*\pi*f_0 = 1/\sqrt(L*C)$,

   where C is C_1 in series with C_2, $1/C = 1/C_1 + 1/C_2$. The aforementioned equation of $\omega_0 = 1/\sqrt(L*C)$ can be obtained from the differential equations resulting from the Conservation of Energy between the capacitor and inductor. That is, energy is transferred between the capacitors' electric field and the inductor's magnetic field (Serway, RA 1992).

3. L_{B1} does not short out the signals through the power supply:

   a) $L_{B1} * \omega_0 \gg 1/(\omega_0 * C_2)$

   b) $L_{B1} * \omega_0 \gg r_\pi$

   c) $L_{B1} * \omega_0 \gg R_2$

4. C_{B1} does connect nodes TP_1 and TP_2: $1/(C_{B1} * \omega_0) \ll R_1$

5. C_{B2} does ground the emitter of the BJT: $1/(C_{B2} * \omega_0) \ll R_E$

6. C_{B2} is not so large such that squegging results in the oscillator. That is, the oscillator begins to squegge.

2.1.6 Small-Signal AC Analysis

At high frequencies, L_{B1} presents a minute amount of admittance to current and becomes an open circuit effectively. Similarly, C_{B1} and C_{B2} become effective short circuits due to their large admittance at high frequencies. Thus, the short circuit at C_{B1} makes the nodes TP_1 and TP_2 to be the same node whilst the short circuit at C_{B2} connects the emitter of the BJT to ground. Assume that the power supply, V_{CC}, becomes a short circuit at these frequencies (Sarkies, K, Cooke, P & Allison, A 2003).
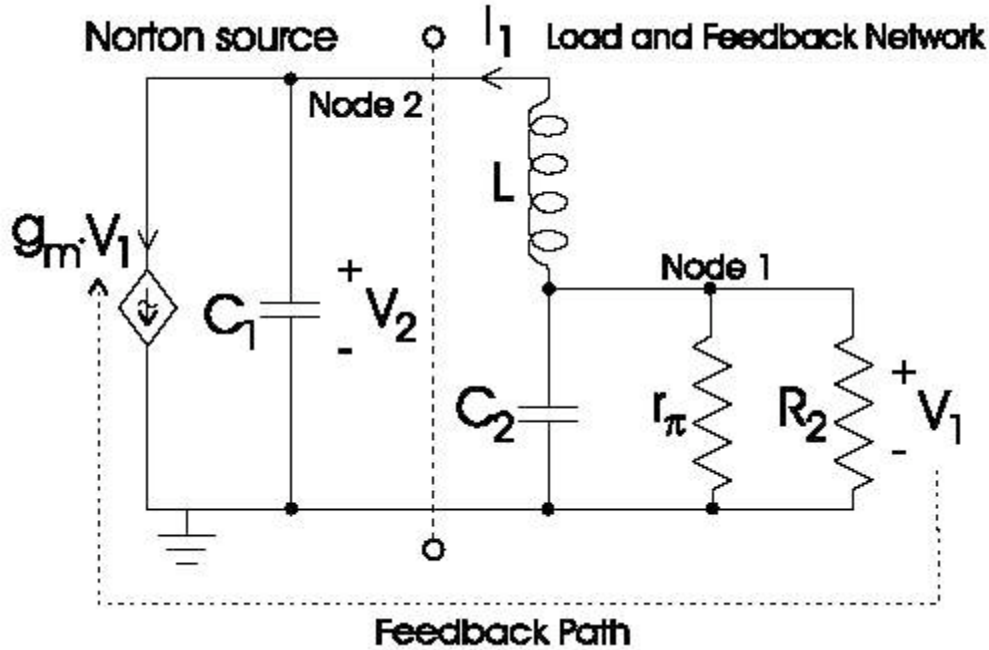
Figure 7. The high frequency or equivalent circuit for the Colpitts Oscillator, shown in Figure 3 (Adapted from Sarkies, K, Cooke, P & Allison, A 2003).

The "hybrid-π" equivalent model of the BJT, see Figure 7, is used to facilitate small-signal AC analysis. In this model, the BJT appears as a controlled Norton current source and as a base emitter resistor r_π, which is related to the forward current gain, β, by $r_\pi = \beta/g_m$ (Sarkies, K, Cooke, P & Allison, A 2003).

Apply a State-Variable approach to obtain the conditions for oscillations in the circuit (Sarkies, K, Cooke, P & Allison, A 2003). The choice of state variables in the electric field is the voltages across the capacitors C_1 and C_2, which are V_1 and V_2 respectively, whilst the choice made in the magnetic field is the current passing through the inductor L, which is I_1. These state variables describe the location of energy in this oscillatory system. The relevant circuit equations for the Colpitts oscillator with state variables $\{V_1, V_2, I_1\}$ are:

Applying nodal analysis at node 1 of Figure 7 yields,

$$I_1 + C_2 * dV_1/dt + V_1 * (1/r_\pi + 1/R_2) = 0 \qquad (1)$$

Similarly, the nodal equation at node 2 of Figure 7 is:

$$-I_1 + C_1 * dV_2/dt + V_1 / g_m = 0 \qquad (2)$$

Applying mesh analysis from node 1 to node 2 through L yields:

$$-V_1 + V_2 + L * dI_1/dt = 0 \qquad (3)$$

Combine Equations (1), (2) and (3) into a single matrix equation:

$$\frac{d}{dt}\begin{bmatrix} V_1 \\ V_2 \\ I_l \end{bmatrix} = \begin{bmatrix} \frac{-1}{C_2}\left(\frac{1}{r_\pi}+\frac{1}{R_2}\right) & 0 & \frac{-1}{C_2} \\ \frac{-g_m}{C_1} & 0 & \frac{+1}{C_1} \\ \frac{+1}{L} & \frac{-1}{L} & 0 \end{bmatrix}\begin{bmatrix} V_1 \\ V_2 \\ I_l \end{bmatrix} \tag{4}$$

Use vector notation to define the matrices $\underline{X}$, A, which is the transitional matrix, and I, which is the identity matrix:

$$\underline{X} = \begin{bmatrix} V_1 \\ V_2 \\ I_l \end{bmatrix} \tag{5}$$

$$A = \begin{bmatrix} \frac{-1}{C_2}\left(\frac{1}{r_\pi}+\frac{1}{R_2}\right) & 0 & \frac{-1}{C_2} \\ \frac{-g_m}{C_1} & 0 & \frac{+1}{C_1} \\ \frac{+1}{L} & \frac{-1}{L} & 0 \end{bmatrix} \tag{6}$$

$$I = \begin{bmatrix} 1 & 0 & 0 \\ 0 & 1 & 0 \\ 0 & 0 & 1 \end{bmatrix} \tag{7}$$

Rewrite Equation (4) in a more compact vector form:

$$\frac{d\underline{X}}{dt} = A\underline{X} \tag{8}$$

Rewrite Equation (8) using matrix notation in the Laplace Domain:

$$(sI - A) \cdot \underline{X} = 0 \tag{9}$$

Equation (9) places a constraint on the permissible values of s.

$$P(s) = \det(sI - A) = |sI - A| = 0 \tag{10}$$

Equation (10) is required to be true to obtain the following characteristic polynomial in s:

$$P(s) = (LC_1 C_2)s^3 + \left(LC_1\left(\frac{1}{r_\pi} + \frac{1}{R_2}\right)\right)s^2 + (C_1 + C_2)s + \left(g_m + \left(\frac{1}{r_\pi} + \frac{1}{R_2}\right)\right) \quad (11)$$

Simplify Equation (11) by defining a variable R, which is equivalent to r_π in parallel with R_2. That is, $1/R = 1/R_2 + 1/r_\pi$. Hence,

$$P(s) = (LC_1 C_2)s^3 + \left(\frac{LC_1}{R}\right)s^2 + (C_1 + C_2)s + \left(g_m + \frac{1}{R}\right) \quad (12)$$

The modes of response of the oscillatory system are of the form exp(λt), where λ are the zeroes of the characteristic polynomial. That is, $P(\lambda) = 0$. For an oscillator, a pair of complex conjugate poles at $\lambda_1 = j\omega_0$ and $\lambda_2 = -j\omega_0$ are required. Hence, conditions for the Colpitts oscillator to oscillate can be derived.

The gain condition is:

$$g_m * R \gg C_2 / C_1 \quad (13)$$

The condition for the output frequency of the oscillator is:

$$\omega_0 = 2\pi f_0 = \frac{1}{\sqrt{L \cdot \left(\frac{1}{\frac{1}{C_1} + \frac{1}{C_2}}\right)}} \quad (14)$$

Simplify Equation (14) by defining a variable C, which is equivalent to C_1 in series with C_2. Hence,

$$\omega_0 = 2\pi f_0 = \frac{1}{\sqrt{L \cdot C}} \quad (15)$$

Thermal voltage, $V_T = k * T/q$ (Rabaey, JM, Chandrakasan, A & Nikolić, B 2003),

where k is the Boltzman constant, $1.38 * 10^{-23}$ J/K, q is the electron charge, $1.6 * 10^{-19}$ C and T is the room temperature in Kelvins.

T = 19.0 °C = 290.15 K was used in the calculations (Refer to Appendices A and B) since the average temperature of Adelaide around noon in April is about 19.0 °C. According to the hourly

history data of Adelaide (*Weather Underground* [Online] 2002), the temperature of Adelaide at 1330 hrs was 19.0ºC on 9 April 2003.

Hence, V ≈ 25 mV (Refer to Appendix B, Section B.1)

It was suggested by Dr. K. Sarkies et al. (2003) to let L = 1 μH, C_{B2} ≈ 680 pF and C_{B2} ≥ 1 μF.

From the calculations of the small-signal analysis in Appendix B,

g_m = 0.64 Ω^{-1}

r_π = 781.25 Ω

L = 1 μH

L_{B1} = 1 mH

C_{B1} = 1 μF

C_{B2} = 680 pF

C_1 = 100 pF

C_2 = 220 pF

2.1.7 PSpice simulation of the circuit.

Change R_1 to 4.7 kΩ, R_2 to 6.2 kΩ and R_E to 330 kΩ.

During the FFT transformation of the PSpice simulation, the 3rd and 4th design specifications, found in Section 2.1.2, were found not to be satisfied. R_1 was changed to 6.8 kΩ and R_E to 470 Ω to meet the design specifications for the frequency and amplitude of the output. The schematic of the Colpitts Oscillator with the changed values is shown in Figure 8.
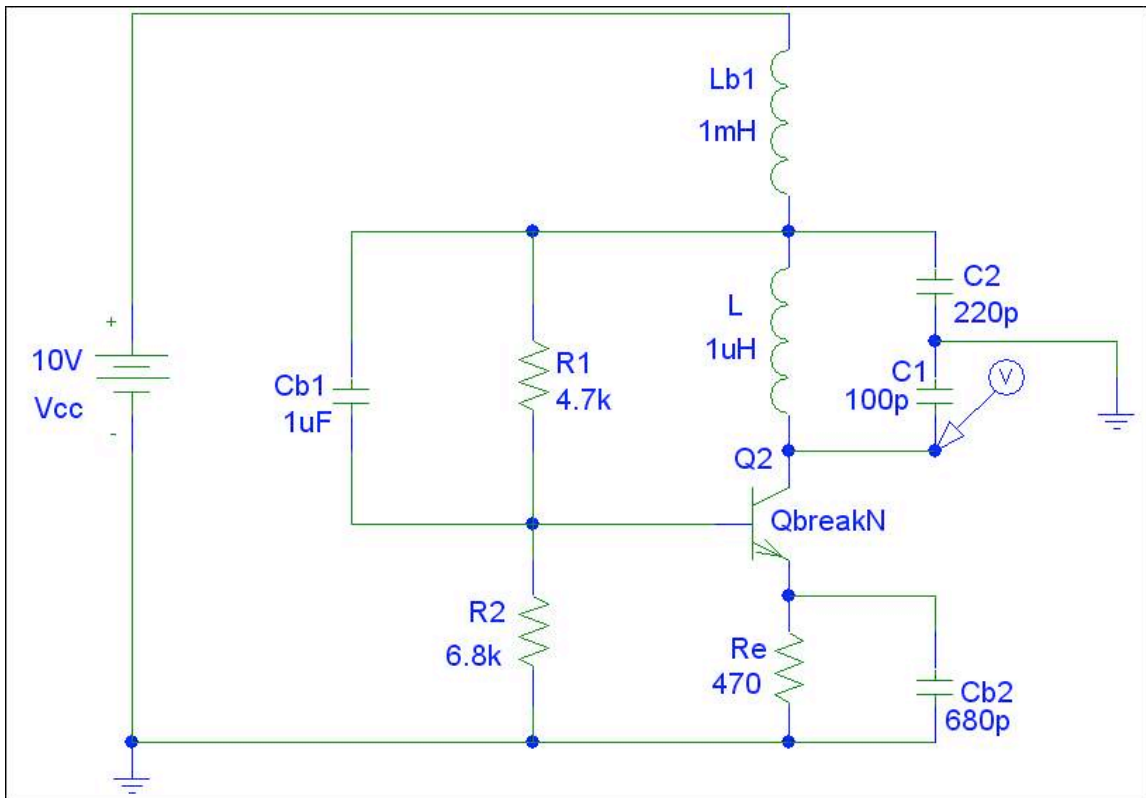

Figure 8. Schematic of the Colpitts Oscillator with the selected values.

The output of the transient simulation is shown in Figure 9. Figure 10 shows an enlargement of the oscillation.
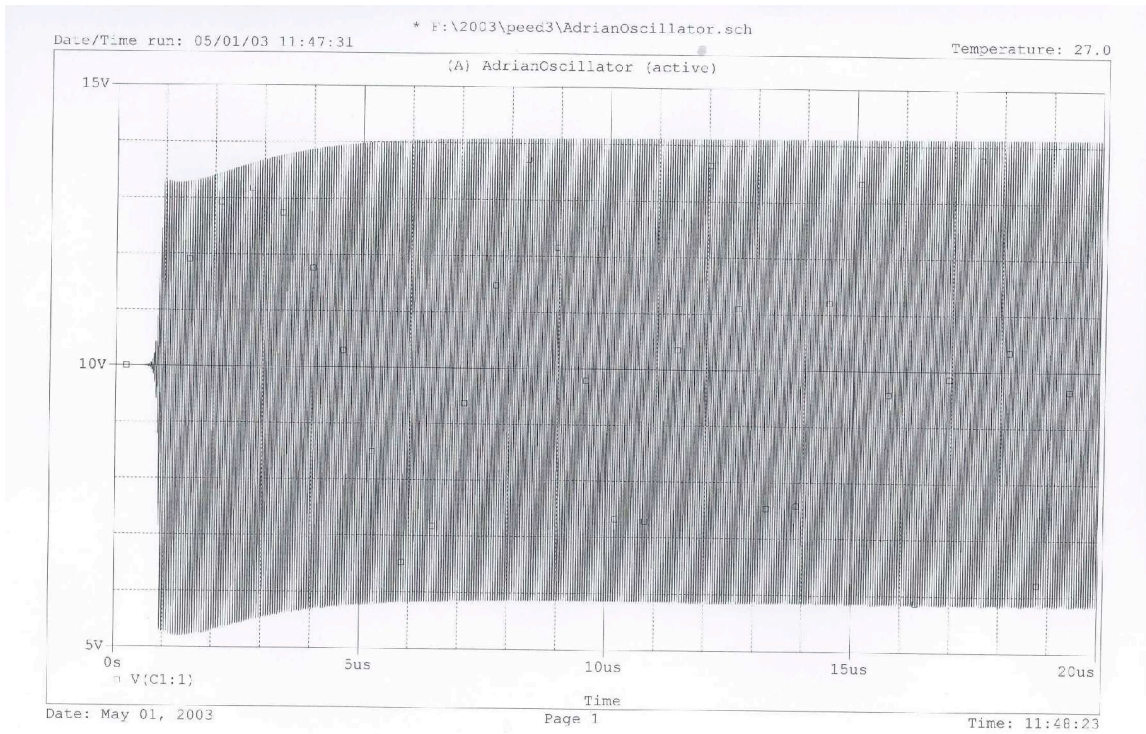
Figure 9. Transient simulation of the Colpitts Oscillator's output.

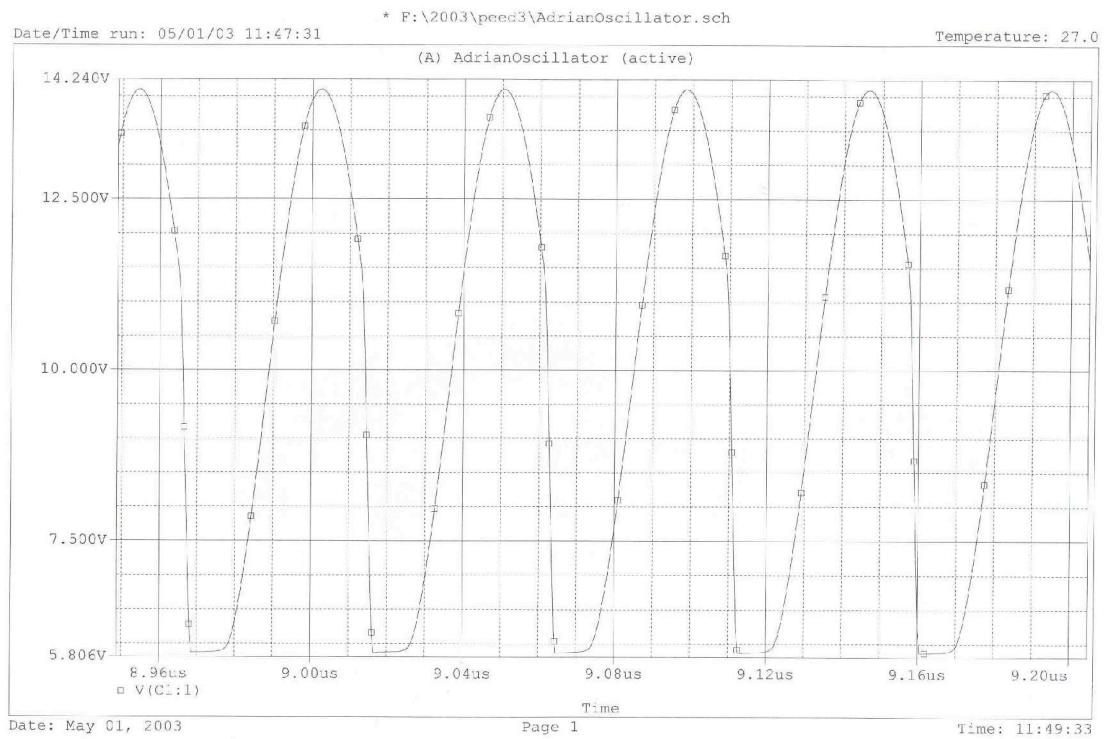Figure 10. Enlargement of the transient simulation of the Colpitts Oscillator's output.

As shown in Figure 11, the Fast Fourier Transform (FFT) shows that the oscillation occurs at about 20.7 MHz, which is close to the desired frequency. Figure 12 shows the FFT for a larger range of frequency values.
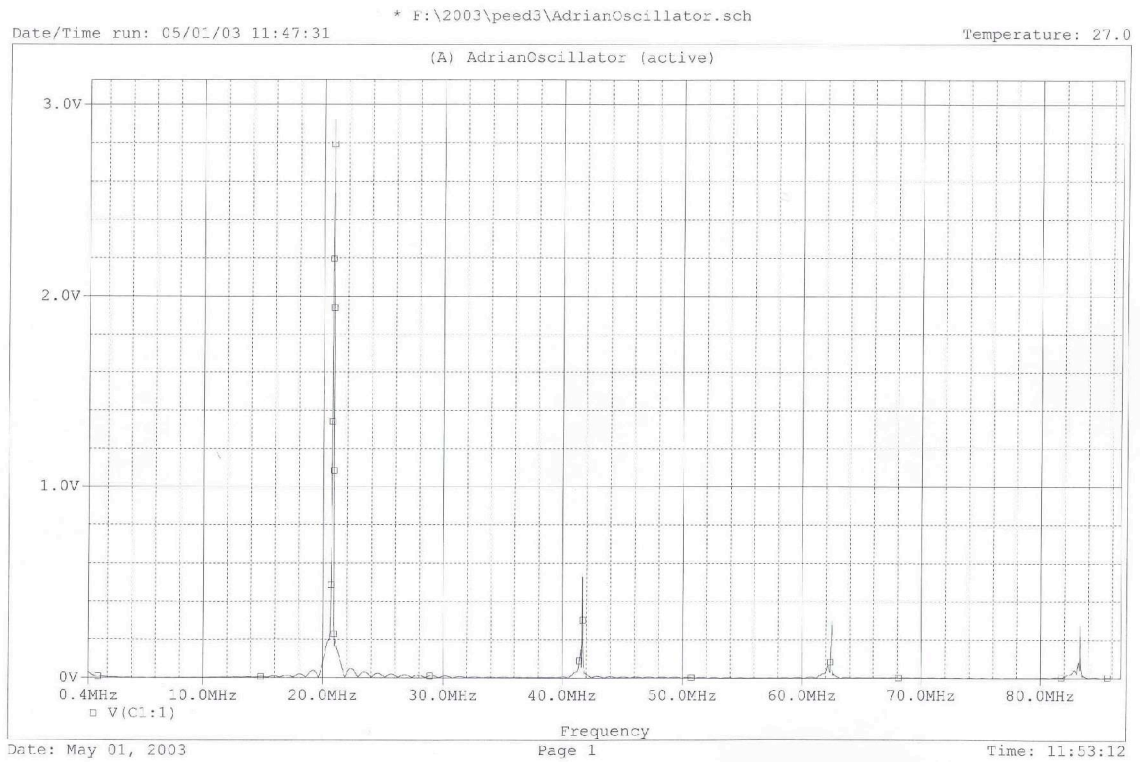

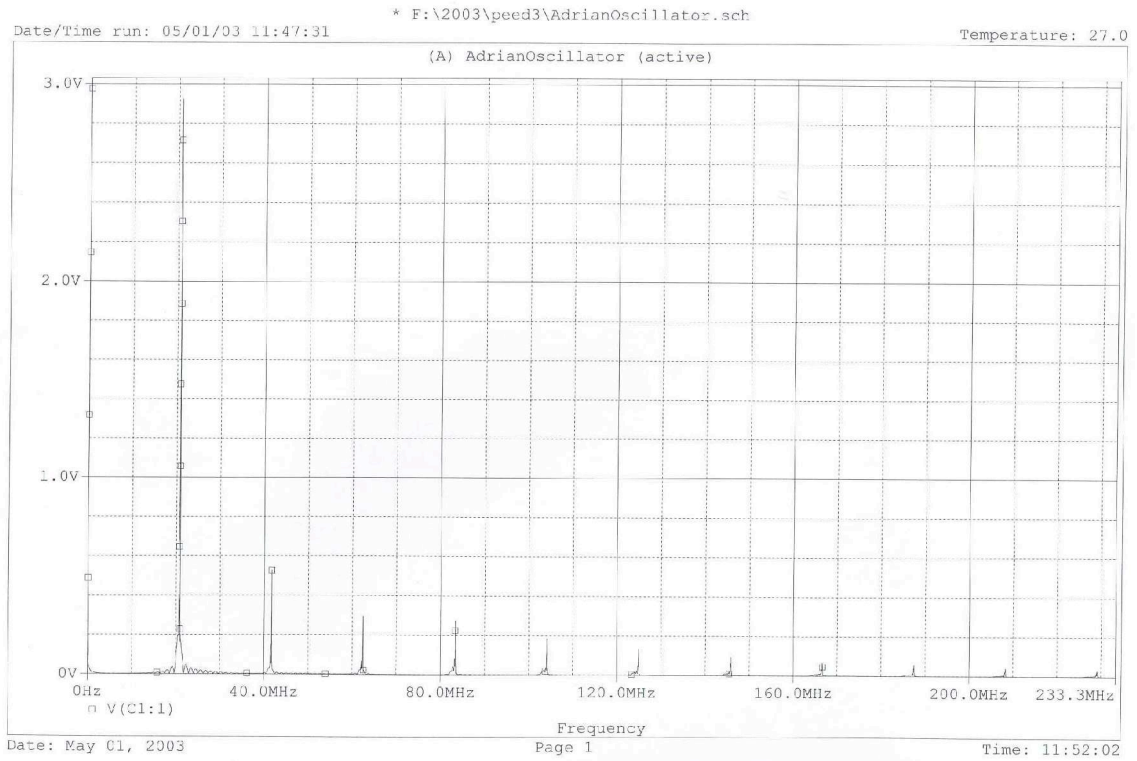Figure 11. The Fast Fourier Transform (FFT) of the Colpitts Oscillator's transient simulation at the output.

(A) AdrianOscillator (active)

Figure 12. The FFT of the transient simulation at the output for a larger range of frequency values.

2.2 Construction of the oscillator

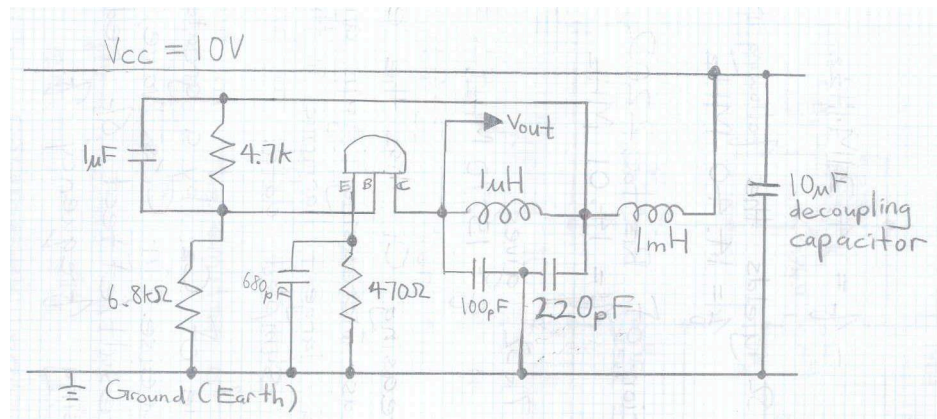### 2.2.1 Measurement of the frequency of oscillation

Figure 13. A rough hand-drawn layout of the Colpitts Oscillator schematic.

A rough hand-drawn layout sketch of the Colpitts oscillator is shown in Figure 13. Upon building the circuit, the measurements for the output voltage, V_0, and the frequency, f, taken from the FFT transformation of the sample data are:

$V_0 = 6.52$ V_{p-p} $\qquad\qquad$ f = 14.21 MHz

Reducing R_E to 390 Ω yields the following readings:

$V_0 = 7.68$ V_{p-p} $\qquad\qquad$ f = 14.40 MHz

Upon further reduction of R_E to 220 Ω,

$V_0 = 9.92$ V_{p-p} $\qquad\qquad$ f = 14.01 MHz

Increasing R_E to 2.7 kΩ gives,

$V_0 = 2.06$ V_{p-p} $\qquad\qquad$ f = 15.70 MHz

Increasing C_2 or decreasing C_1 has the effect of increasing g_m, thus increasing gain and reducing the frequency of the largest harmonic in the FFT transformation of the sampled data.

By reducing the value of C_2 by a greater extent compared to the decrease in C_1's value, it yields an overall result/effect of reducing gain whilst increasing frequency f.

By trial and error, we obtained the following values of v_0 and f by changing R_E to 1.5 kΩ, C_1 to 82 pF and C_2 to 68 pF,

$V_0 = 7.05$ V_{p-p} $\qquad\qquad$ $f_0 = 20.06$ MHz,

where V_0 is the voltage at TP_3 and f_0 is the frequency of oscillation at the output at TP_3. The voltage at TP_2 is 5.12 $V_{p\text{-}p}$ at 20.56 MHz whilst the voltage at the emitter of the BJT is 560 $mV_{p\text{-}p}$ at 20.83 MHz.

2.2.2 Determine the best point to take the measurement of V_0 and f_0

The frequencies measured at the base, collector and emitter differ due to the loading effects of the oscillator probe (HP − 9060) that has been used to take the measurements. The oscillator probe has an input capacitance of approximately 23 pF and an input resistance of 10 MΩ when it is used with Position X10 (EZ Digital n.d.).

Let C_p and R_p represent the input resistance and capacitance of the oscillator probe.

Figure 14.   Schematic of the Colpitts Oscillator, including the capacitance and resistance of the oscillator probe, which is attached to TP_3.

Consider the model of the Colpitts Oscillator circuit with the oscillator probe attached at TP_3, as shown in Figure 14:

C_p and R_p are modelled by placing a capacitor and resistor in parallel with C_1. Since $R_p = 10$ MΩ, it is bypassed and is considered an open circuit. C_p is in parallel with C_1 as indicated in Figure 14. The overall effective capacitance C_1' of C_1 and C_p is:

$$C_1' = C_1 + C_p$$

Thus, the small-signal AC Constraint of $g_m * R > 30 * C_2 / C_1$, found in Section 2.1.5, becomes:

$$g_m * R > 30 * C_2 / C_1', \text{ where } C_1' = C_1 + C_p, C_p \approx 23 \text{ pF}$$

Since the value of R is held constant and $C_1' > C_1$, the value of g_m will decrease. g_m is inversely proportional to C_1, as indicated above, and ω_0 is inversely proportional to C, from the aforementioned equation of $\omega_0 = 1/\sqrt{(LC)}$. C is equal to $(C_1 * C_2)/(C_1 + C_2)$. As C_1 increases, the increase in the numerator $(C_1 * C_2)$ is greater than that of the denominator $(C_1 + C_2)$. ω_0 is equal to $2 * \pi * f_0$. Hence, an increase in C_1 will lead to a decrease in the gain of the circuit as well as the values of g_m and f_0, since C_1 is inversely proportional to g_m and f_0.

The relationship between C_1, g_m and f_0 are verified by observations of the PSpice simulations of the circuit and the changes in the gain/amplitude of the oscillation and the frequency at the output, which are indicated above.

As aforementioned, the increase in C_1, due to the additional capacitance of the probe, leads to a fall in g_m as well as f_0. As a result, the voltage and frequency at TP_3 are lower than they should be.
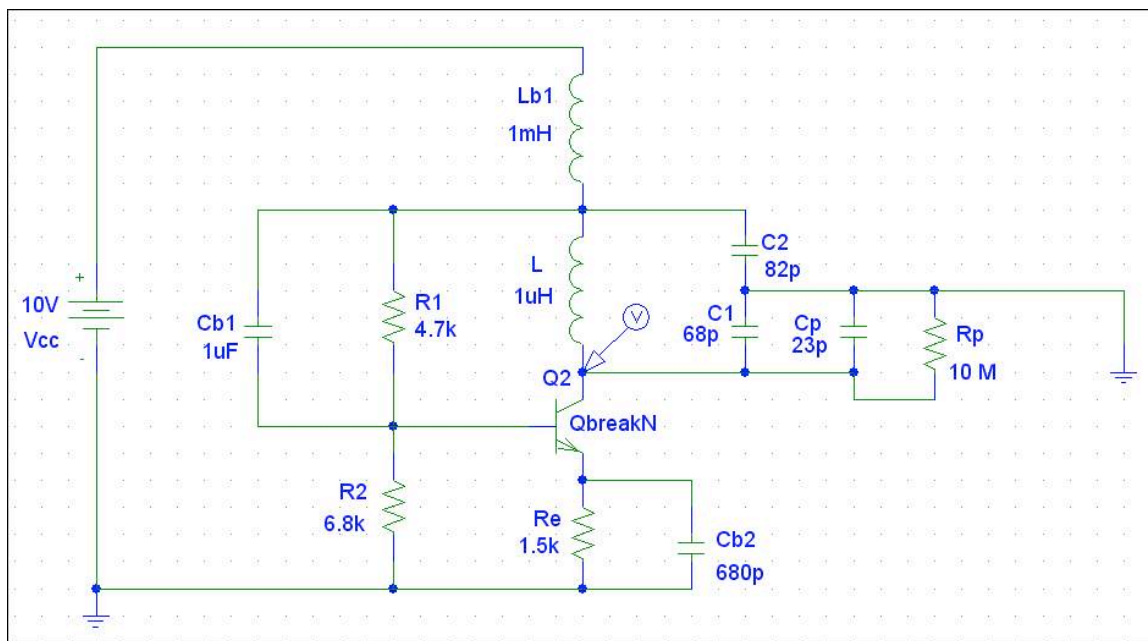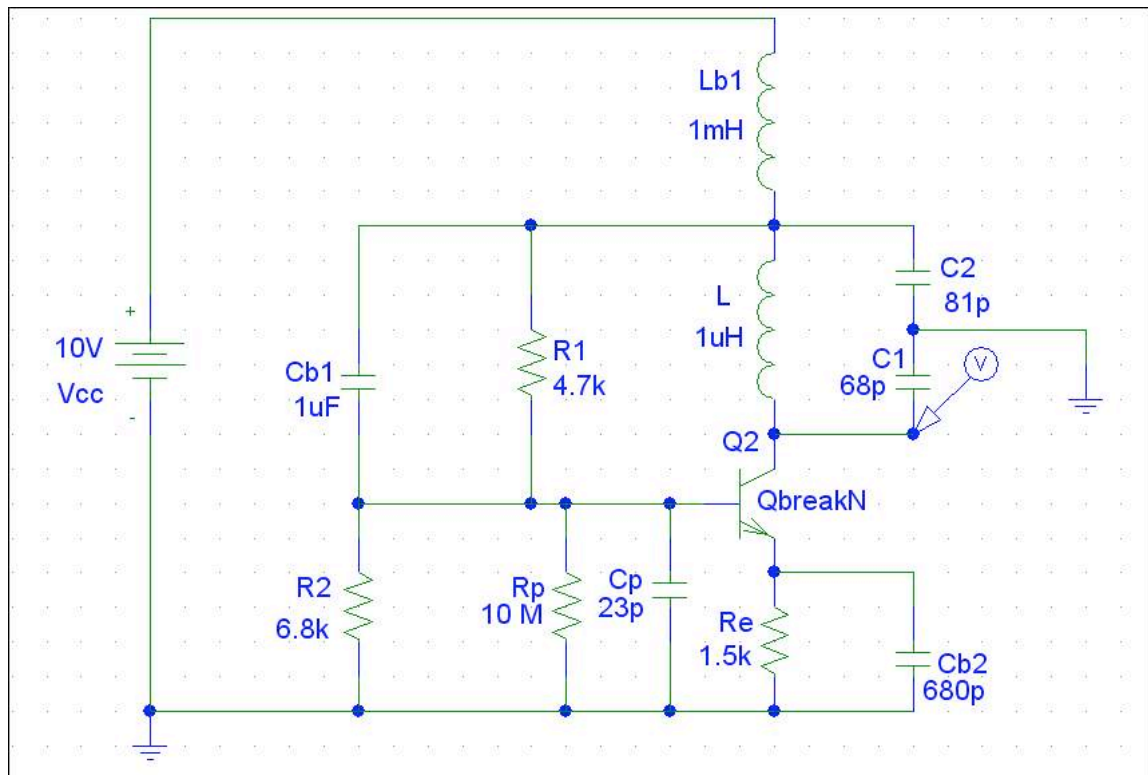

Figure 15.   Schematic of the Colpitts Oscillator, including the capacitance and resistance of the oscillator probe, which is attached to TP_2.

Consider the model of the Colpitts Oscillator circuit with the probe at TP_2, as shown in Figure 15. The small-signal AC Constraint, mentioned in Section 2.1.5, of $g_m * R > 30 * C_2 / C_1$ remains unchanged since the capacitance, C_p, and resistance, R_p, of the probe do not affect R, C_2 or C_1. R_p is bypassed due to its large resistance of 10 MΩ as current always find the path of least resistance. Hence, R_p can be considered an open-circuit. R_2 is in parallel with R_2. Since R_p is an open circuit, R remains unchanged. If $R_p \approx 10$ kΩ, R would have become:

$$R = (R_2 * R_p + r_\pi * R_p + r_\pi * R_2) / (r_\pi * R_2 * R_p)$$

Hence, g_m remains unchanged. This implies that the voltage and frequency at TP_2 would not have been affected by the oscilloscope probe placed at TP_2.

The emitter of the BJT has a much lower voltage than that at its base. That implies that the third specification, found in Section 2.1.2, would not have been met, since the voltage at the emitter of the BJT, 560 mV_{p-p}, is less than that of the desired minimum output voltage of 1 V_{peak}. Note that, C_p would be in parallel with C_{B2}. Since $C_{B2} >> C_p$, the effect of C_p on C_{B2} can be considered to be negligible due to C_p's small capacitance.

Hence, after considering the loading effects of instruments, TP_2 would have been the best point to take the measurement, where the desired amplitude and frequency of oscillation can be best obtained with minimal interference from measuring instruments.

2.2.3   Verify that the specifications and all design constraints have been met

With reference to Appendix C.1, all design specifications have been met. In Appendix C.2, R_l was found to have unacceptable power dissipation whilst all the other DC Bias Constraints were met.

According to Appendix C.3, all except one of the small-signal AC Constraints were met. For L_{B1} not to short out the signals through the power supply, the three constraints concerning L_{B1} must be satisfied. However, the third constraint was not met. This could be due to the large value of R_2. As a result, it may have resulted in unacceptable power dissipation in R_l. A trade-off has to be considered. Reducing R_2 will reduce R, which implies that the amplitude and frequency of oscillation will be lower. This may mean that the design specifications regarding the amplitude and frequency of the oscillator may not be satisfied.

3. Comparison of the nominal and calculated values of L

The nominal value of L is (1.00 ± 0.05) μH, a digital multimeter was used to measure its value, and its calculated value (refer to Appendix D.1 and D.2 for the calculations) is (1.73 ± 0.02) μH. The measured values of the frequency of oscillation, f_0, as well as the capacitances of C_1 and C_2 imply that L should be (1.73 ± 0.02) μH as calculated. This calculated value is significantly different from that of the measured value. This could be due to the parasitic capacitances of the circuit board, which is approximately 10 pF between adjacent connections on the SK10 boards (Allison, A 2002), and/or other electronic components like the resistors and the oscillator probe (as aforementioned in Section 2.2.2) that we did not include in the calculation.

That is, the calculated result of L should be smaller and closer to its nominal value had C included the parasitic capacitances.

4. Relationship between the output frequency of the oscillator and the capacitance of C_1 and C_2

The capacitance of C_1 was kept constant and C_2's value was trimmed by placing other capacitors in parallel with it. It was observed from the experimental results (refer to Table 1) that as C_1's value increased, the amplitude and the frequency of oscillation decreased.

Table 1. Measured values of V_0 and f_0 due to a change in C_1

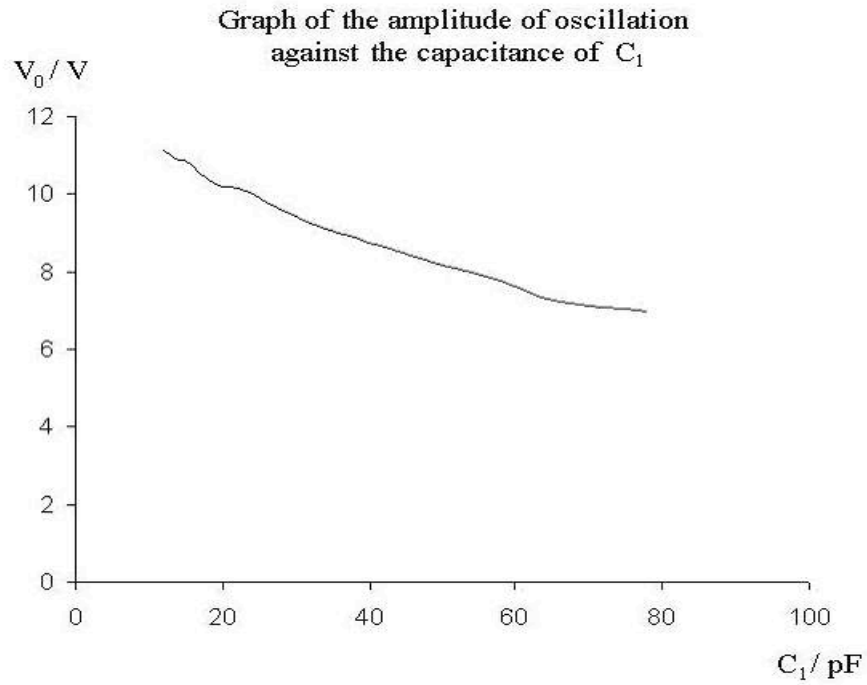| C_1 / pF	V_0 / V	f_0 / MHz
12	11.15	27.87
14	10.88	27.07
15	10.84	26.66
19	10.26	25.75
23	10.08	24.83
29	9.52	23.85
34	9.12	23.14
42	8.64	22.13
50	8.16	21.37
58	7.76	20.77
66	7.22	20.06
78	6.96	19.93

Figure 16. Graph of the amplitude of oscillation, V_0, against the capacitance of C_1.
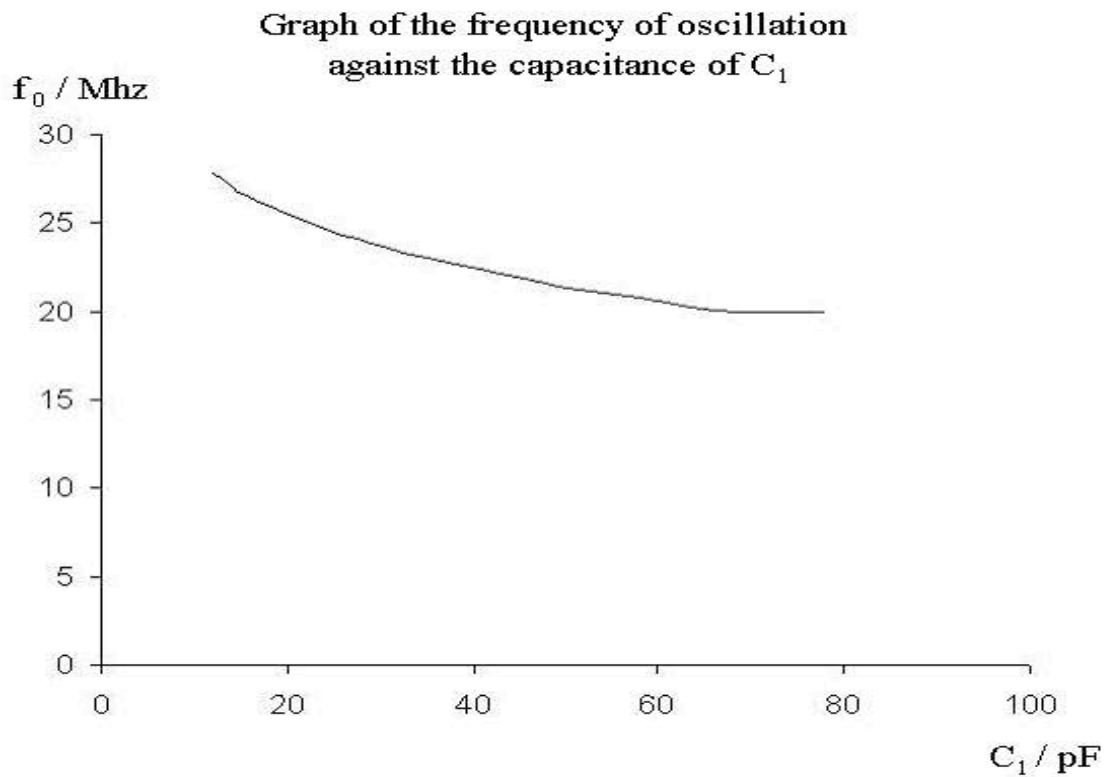

Figure 17. Graph of the frequency of oscillation, f_0, against the capacitance of C_1.

The gain of the oscillator and the amplitude of oscillation are inversely proportional to the capacitance of C_1. Hence, a graph of C_1 against V_0 should look like a rectangular hyperbola in the first quadrant (*MathWorld.Wolfram.com* [Online] 2003). However, the graph of the experimental data of C_1 and V_0, shown in Figure 16, seem to indicate otherwise. Since $C = C_2 * C_1 / (C_2 + C_1)$ and C has an inverse square relationship with f_0 ($\omega_0 = 2*\pi*f_0 = 1/\sqrt{(L*C)}$), considering C_2 as a constant, C_1 and f_0 should share an inverse square relationship as well. However, the graph of the measured values of C_1 and f_0, shown in Figure 17, seem to indicate otherwise.

This could be due to the capacitance of 10 pF between adjacent connections of the SK10 board (Allison, A 2002) and 23 pF in parallel with C_1 due to the oscilloscope probe (EZ Digital n.d.). Had these capacitances been taken into account, the graphs shown Figure 16 and Figure 17 would have resembled ideal curves indicating a rectangular hyperbola in the first quadrant and an inverse square relationship.

5   Squegging Oscillator

C_{B2} was increased to 100 nF and the base-emitter voltage, V_{BE}, is observed. The oscillator was observed to be squegging. Squegging is defined as a choking type of cut-off action in a circuit caused by large signals whilst the squegging oscillator is defined as an oscillator that starts and tops oscillating intermittently due to squegging (Turner, RP & Gibilisco, S 1998).

The waveforms of V_B and V_E were superimposed on each other using the digital oscilloscope. The display panel, as shown in Figure 18, indicated where the oscilloscope and squegging starts. V_{BE} ($V_{BE} = V_B - V_E$) was measured at the start of oscillation and was found to be 0.64 V. V_{BE} is measured to be -1.44 V at the start of squegging.
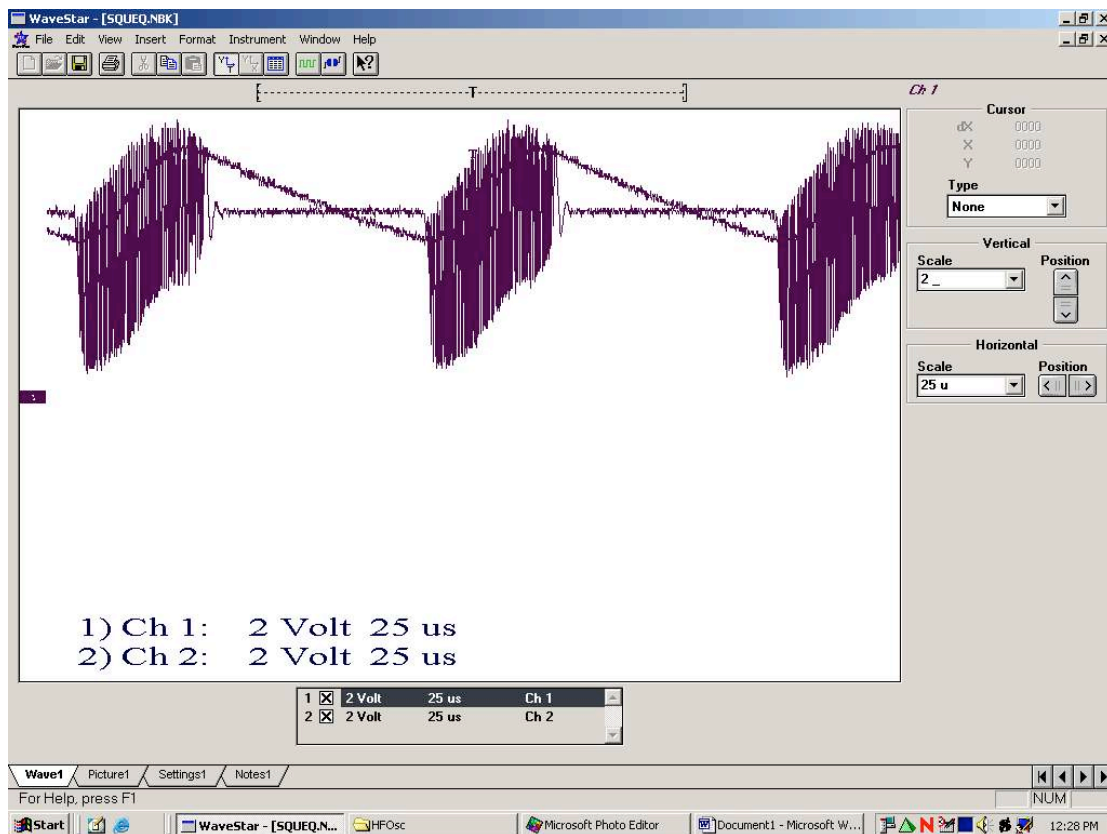

Figure 18. Display of the digital oscilloscope showing V_B superimposed on V_E.

When V_{BE} is greater than 0.64 V, the BJT is in the linear mode of operation and is considered a short circuit as it conducts. As a result, C_{B2} charges up and oscillation occurs. This also causes V_E

to increase and exceed V_B, as well as V_0. When V_{BE} is less than 0.64 V, the BJT is in the cut-off mode of operation and it becomes an open circuit. Thus, the BJT stops conducting and switches off. The oscillation stops and squegging occurs. This causes C_{B2} to discharge and V_E, which is the voltage across the capacitor C_{B2}, to fall.

Once V_{BE} reaches a minimum value of 0.64 V again, as V_E falls, the oscillations start again and the process is repeated. This switching on and off of the BJT results in switching on and off of the Colpitts oscillator. That is, when V_E exceeds V_B, the oscillator is choked/cut-off because the BJT, which is in the cut-off mode of operation, has no feedback.

6 Purity of signals at different points in the circuit

C_{B2} was replaced with its original value, which is measured to be 66 pF. By using the FFT feature of the digital oscilloscope, the spectral characteristics of the signal from the oscillator, shown in Figure 19, were measured to indicate the purity of the signals at different points in the circuit. Substantial spectral lines resulting from harmonics of the distorted signal were sought. The percentage total harmonic distortion (%THD) is used to indicate the purity of a signal by measuring the extent to which a pure signal is distorted. %THD is defined as (Bogner, RE 1992):

%THD = (mean power of all distortion components) / (mean power of total distortion signal + distortion) * 100%

$\%THD = \sqrt{((C_2)^2 + (C_3)^2 + (C_4)^2 + (C_5)^2 + \ldots)} / C_1 * 100\%$,

where C_n, where n is an integer indicating the nth harmonic, is the ratio of $P_n/P_1 = (V_n / V_1)^2 = 10^{(\Delta dB) / 10(dB))}$ (Sarkies, K, Cooke, P & Allison, A 2003)
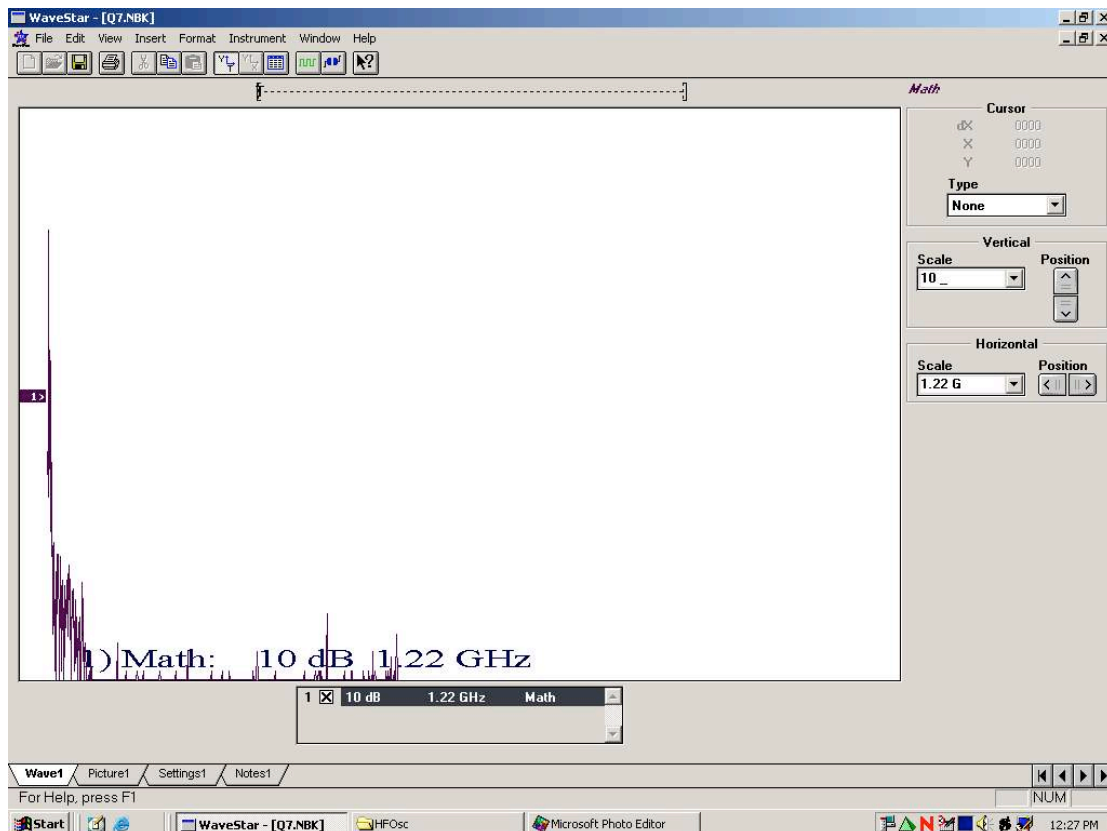

Figure 19. The display of the spectral characteristics of the output signal of the Colpitts Oscillator.

Table 2. Values of the harmonics and the corresponding frequency for the FFT taken at TP_3

C_n / no units	f / MHz
66	20.0
47	40.0
38	60.0
30	82.0
22	102.0
19	302.0
18	162.0

In the context of radio, with incoming signals passing through a Radio Frequency filter, the most significant unwanted feature of the output signal from the Colpitts oscillator is the harmonic at 40 MHz, since its value is very close to that of the fundamental harmonic at 20 MHz. The % THD of TP_3 is 1.24% (the calculations are shown in Appendix E.1 using the values indicated in Table 2).

Table 3. Values of the harmonics and the corresponding frequency for the FFT taken at TP_2

C_n / no units	f / MHz
64	20.0
51	40.0
40	60.0
36	80.0
22	136.0
22	100.0
20	120.0

As shown in the calculations in Appendices E.2 and E.3 (Refer to Tables 3 and 4 for the values of the harmonics at TP_2 and the emitter), the %THD at TP_2 is 1.29% and that at the emitter of the BJT is 1.50%.

Table 4. Values of the harmonics and the corresponding frequency for the FFT taken at the emitter of the BJT

C_n / no units	f / MHz
62	20.0
50	60.0
45	80.0
38	100.0
34	120.0
34	36.0
19	236.0

Of the three different points of the Colpitts oscillator circuit where the purity of the signals were measured, TP_3 has the smallest %THD at 1.24% whilst the emitter of the BJT has the largest

%THD at 1.50%. This is because the power supply, V_{CC}, as well as C_{B1} and C_{B2} are considered to be short-circuited at high frequencies. Since the connection of the emitter of the BJT to ground via the emitter resistor is poor, small voltage signals due to the electromagnetic interference of the surrounding electronic equipment, such as the digital oscilloscope, are present at the ground connections of the SK10 circuit boards. Hence, these small voltage signals are propagated to the emitter of the BJT as well as the base of the BJT, which are the TP_1 and TP_2 connections, through the short circuit present at V_{CC}, C_{B1} and C_{B2}. Hence, the %THD at the emitter and TP_2 are higher than that at TP_3, which has the inductor L that is a storage component reducing the noise at TP_3.

7 Minimisation of effects on oscillator operation caused by external circuits

A common collector buffer amplifier, also known as the emitter follower buffer, is designed, built and connected to TP_3 as a possible means of minimising the effect of external circuits on the oscillator operation. This is an effective solution since interactions between the oscillator and load are reduced. The matches the low impedance of the load and buffers the signal source that has a high output impedance. This implies that the input impedance of the load would be high in the absence of the emitter follower buffer. Hence, the signal source of the load would not have to "work so hard" (*HyperPhysics* [Online] 2000). A Colpitts oscillator that has high output impedance is unable to drive a load with low input impedance due to loading effects (Davis, BR 1997).

The common collector buffer amplifier is also called the emitter follower since this impedance matching device takes its output from the emitter resistor. (*HyperPhysics* [Online] 2000).

Since TP_3 is connected to the buffer's high input impedance, the buffer has little effect on the operation of the oscillator as the loading effects of the load are minimised. Changes in the output load cannot be reflected back to the oscillator as the output of the buffer is connected to an external load. The voltage gain of the emitter follower is slightly less than unity since the voltage of the buffer's emitter is constrained by the voltage drop of approximately 0.6 V ($V_{BE} \approx 0.6$ V) across the base-emitter junction. Note that its function is not that of a constant voltage gain but of constant current or power gain and matching impedances (*HyperPhysics* [Online] 2000).
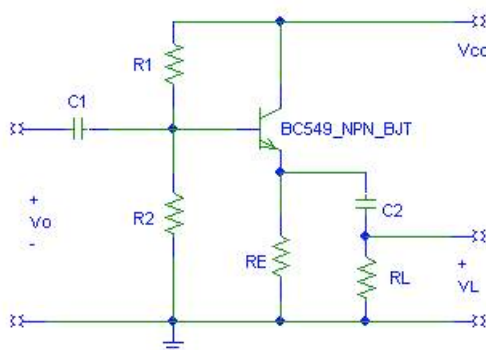

Figure 20. Schematic for the common collector buffer amplifier (*HyperPhysics* [Online] 2000).

Figure 20 shows a schematic of a possible emitter follower design. With reference to Appendix F.1, the calculated values of R_E, R_1, R_2, C_1 and C_2 are as follows:

$R_E = 2.2 \text{ k}\Omega$

$R_1 = 10 \text{ k}\Omega$

$R_2 = 22 \text{ k}\Omega$
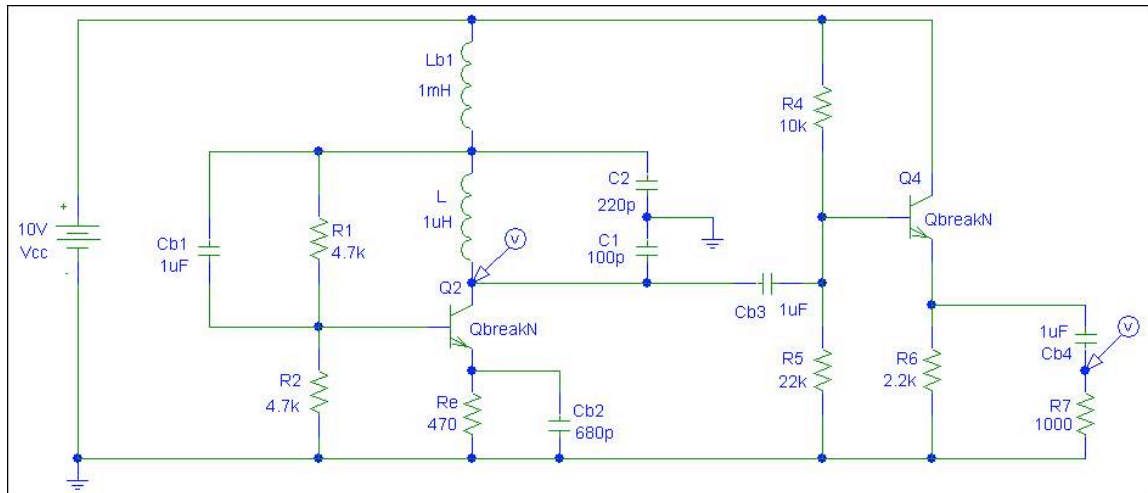
$C_1 = C_2 = 1 \text{ } \mu\text{F}$

Figure 21. The Colpitts oscillator with a common collector buffer amplifier attached to its output.

Figure 21 shows how the common collector buffer amplifier is attached to the output of the Colpitts oscillator. The voltage at the load resistor is 1.22 V_{peak} at 19.95 MHz. Clearly, the emitter follower circuit as failed to work as a buffer. Values of R_E of the oscillator and the buffer as well as R_1, R_2 and R_E of the oscillator were changed through experimental trial and error to obtain a "unity" gain.

The following values of the Colpitts oscillator were changed:

$R_E = 3.29 \text{ k}\Omega$

$R_1 = 2.17 \text{ k}\Omega$

$R_2 = 4.6 \text{ k}\Omega$

The value of the emitter's resistor in the buffer amplifier circuit was changed to 1.49 kΩ. The voltage of the load was measured to be 4.72 V at 20.62 MHz. The voltage at the output of the oscillator was measured at 4.96 V at 20.62 MHz. Note that the voltage at the load is slightly less than the output voltage of the oscillator as aforementioned due to the voltage drop of 0.6 V across the PN junction of the buffer amplifier's BJT.

It was observed that during the measurement of the frequency at the output, the frequency was observed to be fluctuating within a range of about 0.2 MHz. The frequency stability of an oscillator is defined by Millman, J & Halkias, CC (1967) to be a measure of the oscillator's ability

to maintain a fixed frequency over a long time interval. Since the design of the oscillator is limited by the onset of the non-linearity mode of operation in the active devices associated with the capacitor, the amplitude of the oscillator was decreased to reduce the significance of the non-linearity due to device capacitances and loss resistance. This kept the gain of the buffer amplifier to be as close to one as possible. A unity gain is unachievable in practice due to the voltage drop across the base-emitter junction of the buffer amplifier's BJT as well as the change in the circuit components and transistors characteristics due to age, temperature and the voltage drop across them. It is of interest to note that the transistors' parameters are inherently unstable and stray circuit elements and couplings, which magnitudes can only be estimated, are difficult to locate.

8. Conclusion

As suggested by Sarkies Cooke & Allison (2003) as well as Sydenham (1983) and Sedra & Smith (1998), a proper gain of the feedback oscillatory system, as shown in Figure 2, is desired to produce oscillations of amplitudes greater than 1 V_{peak} at the desired frequency of 20 MHz. Suitable component values were chosen and calculated as indicated in Appendices A and B for the suggested oscillator circuit, the Colpitts oscillator. During this design process, the fundamental concepts of positive feedback and stability in Control theory were revisited whilst selecting the gain of the oscillator, $g_m * R$, to be much greater than C_2 / C_1.

Other concepts, such as Radio Frequency transmission and signals and spectra were also covered in this experiment. The relationship of the frequency of oscillation with respect to the values of storage components was examined and the concept of parasitic capacitances present in the SK10 circuit board and the measuring instruments, such as the oscilloscope probe, was introduced.

The concept of squegging was considered when the oscillator started and stopped intermittently. It was found that by increasing the value of C_{B2}, the oscillator would oscillate as the BJT switches on and off due to the charging and discharging of C_{B2}. Spectral characteristics of the signals at various points of the circuit were measured to find out how the operation of the oscillator was affected by the measuring instruments, circuit components and circuit board.

Lastly, loading effects of external circuits were considered, as a common collector buffer amplifier was designed and built to decrease the interactions of the Colpitts oscillator and the load.

9. References

9.1 Books

Franco, S 1995, *Electrical Circuit Fundamentals*, Saunders College Publishing, Orlando, Florida

Hambley, AR 2000, *Electronics*, Second International Edition, Prentice-Hall International, Inc., Upper Saddle River, New Jersey

Millman, J & Halkias, CC 1967, *Electronic Devices and Circuits*, International Student Edition, McGraw-Hill Book Company/Kōgakusha Company, LTD, Tokyo

Rabaey, JM, Chandrakasan, A & Nikolić, B 2003, *Digital Integrated Circuits: A Design Perspective*, Second International Edition, Pearson Education International, Upper Saddle River, New Jersey

Schwarz SE & Oldham, WG 1993, *Electrical Engineering: An Introduction*, Second International Edition, Saunders College Publishing, Orlando, Florida

Sedra, AS & Smith, KC 1998, Microelectronic Circuits, Oxford University Press, Oxford

Serway, RA 1992, *Physics for Scientists and Engineers*, Third Edition, Updated Version, Saunders College Publishing, Orlando, Florida

Sydenham, PH 1983, *Electronics – It's easy Vol. 1*, The Federal Publishing Company, Sydney.

Turner, RP & Gibilisco, S 1998, *The Illustrated Dictionary of Electronics*, Fourth Edition, Tab books, Inc, Blue Ridge Summit, PA, United States

9.2 Papers

Allison, A 2002, *Experimental Electrical Engineering III Lecture 2: Construction techniques for Solder-less (SK10) prototyping boards*, the University of Adelaide, Adelaide

Bogner, RE 1992, *Signals and Spectra*, the University of Adelaide, Adelaide

Davis, BR 1997, *Experimental Electrical Engineering II*, the University of Adelaide, Adelaide

Sarkies, K, Cooke, P & Allison, A 2003, *ELEC ENG 3019 A/B Practical Electrical and Electronic Design III High Frequency Oscillator*, the University of Adelaide, Adelaide

9.3 Component Data Sheets/Product Specifications

EZ Digital n.d., *Oscilloscope Probe Kit Model. HP-9060*, EZ Digital, Puchon-Si, Kyonggi-do, Korea

Philips Semiconductors 1999, *Discrete Semiconductors: BC549; BC550 NPN general-purpose transistors*, Philips Semiconductors, Eindhoven, The Netherlands

9.4 Online databases

MathWorld.Wolfram.com [Online] 2003. Available: Mathematics: Plane Curves: Conic Section, viewed on 15 May 2003. Available from

<http://mathworld.wolfram.com/RectangularHyperbola.html>

SearchNetworking.com [Online] 2003. Available: Definitions, viewed on 13 May 2003. Available from <http://searchnetworking.techtarget.com/sDefinition/0,,sid7_gci331643,00.html>

Weather Underground [Online] 2002. Available: Adelaide, South Australia: History for Adelaide, SA: Hourly history data for 9 April 2003, viewed on 12 May 2003. Available from <http://www.wunderground.com/history/station/94672/2003/5/1/DailyHistory.html>

HyperPhysics [Online] 2000. Available: Electricity and Magnetism: Electronic Concepts: Feedback Concepts: Emitter Follower: Emitter Follower Buffer, viewed on 16 May 2003. Available from <http://hyperphysics.phy-astr.gsu.edu/hbase/electronic/emitfol.html#=3>

Appendix A   DC Bias Calculations

A.1   Relationship between I_C and I_E

Since β, the DC current gain $= 500$, $I_E = (\beta + 1)/\beta * I_C$

Therefore, $I_C \approx I_E$ since $(500 + 1)/500 \approx 1$

Hence, $I_C \approx I_E = V_E/R_E$

A.2   Find the values of V_{CE}, V_E and V_B

Let $V_{CC} = V_C$

$V_{CC} = 10.0$ V (see Section 2.1.2)

$V_{CE} = \frac{1}{2}V_{CC}$

$\quad\quad = \frac{1}{2} * 10$ V

$V_{CE} = 5$ V

$V_{CE} = V_{CC} - V_E$

$V_E \quad = V_{CC} - V_{CE}$

$\quad\quad = 10$ V $- 5$ V

$V_E \quad = 5$ V

$V_{BE} = V_B - V_E$

$V_B \quad = V_E + V_{BE}$

$\quad\quad = 5$ V $+ 0.6$ V

$V_B = 5.6$ V

A.3   Find the ratio of R_1/R_2

$R_1/R_2 \quad = V_{CC} / V_B - 1$

$\quad\quad\quad = 10$ V $/ 5.6$ V $- 1$

$R_1/R_2 \quad = 0.7857$

A.4   Find the limits of I_C, R_E, R_1 and R_2

Assume that the BC549 NPN BJT will not dissipate more than 125 mW of power, as aforementioned in the DC Bias Constraints (See Section 2.1.3).

$I_C \quad \leq P_{max} / V_{CE}$

$\quad\quad \leq 0.125$ W $/ 5$ V

$I_C \quad \leq 0.025$ A

$$(V_E)^2 / R_E \leq P_{max}$$

$$R_E \geq (V_E)^2 / P_{max}$$

$$\geq (5\ V)^2 / 0.125\ W$$

$$R_E \geq 200\ \Omega$$

$$(V_{CC} - V_B)^2 / R_1 \leq P_{max}$$

$$R_1 \geq (V_{CC} - V_B)^2 / P_{max}$$

$$\geq (10\ V - 5.6\ V)^2 / 0.125\ W$$

$$R_1 \geq 154.88\ \Omega$$

$$(V_B)^2 / R_2 \leq P_{max}$$

$$R_2 \geq (V_B)^2 / P_{max}$$

$$\geq (5.6\ V)^2 / 0.125\ W$$

$$R_E \geq 250.88\ \Omega$$

A.5   Find the values of I_C, I_E, I_B, I_{ch}, R_E, R_1 and R_2

Use P_{max} = 80 mW (See Section 2.1.4 for reasons why this value was chosen) to work out the values of I_C, I_E, I_B, I_{ch}, R_E, R_1 and R_2.

$$I_C = P_{max} / V_{CE}$$

$$= 0.08\ W / 5\ V$$

$$I_C = 16\ mA$$

Since $I_C \approx I_E$, $I_E \approx 16$ mA

$$I_B = I_C / \beta$$

$$= 16\ mA / 500,\ \text{since } \beta = 500,\ \text{as aforementioned in Section 2.1.4}$$

$$I_B = 32\ \mu A$$

$$I_{ch} = 30 * I_B$$

$$= 30 * 32\ \mu A$$

$$I_{ch} = 0.96\ mA$$

$$R_E = (V_E)^2 / P_{max}$$

$$= (5\ V)^2 / 80\ mW$$

$$R_E = 312.5\ \Omega$$

$R_1/R_2 = 0.7857$

$\therefore \quad R_1 = 0.7857*R_2$

$I_{ch} \quad = V_{CC} / (R_1 + R_2)$

$\quad = V_{CC} / (0.7857*R_2 + R_2)$

$\quad = V_{CC} / (1.7857 * R_2)$

$R_2 \quad = V_C / (1.7857 * I_C)$

$\quad = 10 \text{ V}/ (1.7857 * 0.96 \text{ mA})$

$R_2 \quad = 5.83 \text{ k}\Omega$

$\therefore \quad R_1 = 0.7857*5.83 \text{ k}\Omega$

$R_1 \quad = 4.58 \text{ k}\Omega$

Appendix B   Calculations for AC analysis

B.1   Find the value of V_T

Take T = 290.15 K for reasons aforementioned in Section 2.1.6

V_T = k * T/q

    = $(1.38*10^{-23} * 290.15/(1.6*10^{-19}))$ V

    = 25.025 mV

V_T ≈ 25 mV

B.2   Find the values of g_m and r_π

$g_m = i_c / V_{BE}$

The application of the Shockley equation to the base-emitter P-N junction yields,

$$g_m \approx I_C / V_T$$

∴ $g_m \approx$ 16 mA / 25 mV

$g_m \approx 0.64\ \Omega^{-1}$

$r_\pi = V_T / I_B = \beta / g_m = 500 / 0.64\ \Omega^{-1}$

$r_\pi = 781.25\ \Omega$

B.3   Find the value of ω_0

f_0 = 20 MHz, as aforementioned in the Section 2.1.2

$\omega_0 = 2 * \pi * f_0 = 2 * \pi * 20$ MHz = 125.66 M rads^{-1}

B.4   Find the value of L and L_{B1}

Select L = 1 µH, see Section 2.1.6.

$L_{B1} * \omega_0 > 30 * r_\pi$

$L_{B1} > 30 * r_\pi / \omega_0$

$L_{B1} > 30 * 781.25\ \Omega / 125.66$ M rads^{-1}

$L_{B1} > 186.5$ µH

$L_{B1} * \omega_0 > 30 * R_2$

$L_{B1} > 30 * R_2 / \omega_0$

$L_{B1} > 30 * 5.83$ kΩ / 125.66 M rads^{-1}

$L_{B1} > 1.39$ µH

The only values of inductors available in the laboratory are 1 mH and 1 μH. Hence, choose $L_{B1} = 1$ μH

B.5 Find the values of the bypass capacitors C_{B1} and C_{B2}

$R_1 > 30 / (C_{B1} * \omega_0)$

$C_{B1} > 30 / (R_1 * \omega_0)$

$C_{B1} > \{ 30 / (4.58 \text{ k}\Omega * 125.66 \text{ M rads}^{-1}) \}$ F

$C_{B1} > 52.1$ pF

Choose $C_{B1} = 1$ μF, as aforementioned in Section 2.1.6.

$C_{B2} > 30 / (R_E * \omega_0)$

$C_{B2} > \{ 30 / (3.125 \Omega * 125.66 \text{ M rads}^{-1}) \}$ F

$C_{B2} > 764$ pF

Choose $C_{B2} = 680$ pF, as aforementioned in Section 2.1.6, even though C_{B2} is less than 764 pF.

B.6 Find the values of R and C

$\omega_0 = 1/ \sqrt{(L * C)}$

$L*C = 1/ (\omega_0)^2$

$C = 1/ \{L*(\omega_0)^2\}$

$= (1$ μF $* (125.66 \text{ M rads}^{-1})^2)^{-1}$ F

$C = 63.3$ pF

$R = (1/r_\pi + 1/R_2)^{-1} = R_2 * r_\pi / (R_2 + r_\pi)$

$= 5.83 \text{ k}\Omega * 781.25 \Omega / (5.83 \text{ k}\Omega + 781.25 \Omega)$

$R = 688.9 \Omega$

B.7 Find the limits and values of C_1 and C_2.

$L_{B1} * \omega_0 > 30/(\omega_0 * C_2)$

$C_2 > 30/((\omega_0)^2 * L_{B1})$

$C_2 > (30/((125.66 * 10^6)^2 * 0.001))$ F

$C_2 > 1.90$ pF

Choose $C_2 = 220$ pF

$g_m * R > 30 * C_2/C_1$

$C_1 > 30 * C_2 / (g_m * R)$

$C_1 > 30 * 220 \text{ pF} / (0.64 \ \Omega^{-1} * 688.9 \ \Omega)$

$C_1 > 15.0 \text{ pF}$

$C = (1/C_1 + 1/C_2)^{-1}$

$\therefore \quad 1/C_1 = 1/C - 1/C_2$

$C_1 = (1/C - 1/C_2)^{-1}$

$\therefore \quad C_1 = [(C_2 - C) / (C * C_2)]^{-1}$

$C_1 = (C * C_2) / (C_2 - C)$

$\therefore \quad C_1 = (63.3 \text{ pF} * 220 \text{ pF}) / (220 \text{ pF} - 63.3 \text{ pF})$

$C_1 = 88.9 \text{ pF}$

Choose $C_1 = 100$ pF since the smallest capacitor value that is greater than 88.9 pF is 100 pF.

Appendix C   Verification of design specifications and constraints

C.1   Verifying design specifications

A regulated laboratory DC power supply is used to set V_{CC} at 10 V. The output frequency, f_0, is measured at 20.06 MHz, which is within the specified range of (20.00 ± 0.20) MHz. The output voltage is measured at 3.52 V_{peak}, which is greater than the minimum required value of 1 V_{peak}.

Hence, with reference to Section 2.1.2, all design specifications are met.

C.2   Verifying DC constraints

I_E = V_E / R_E, according to Ohm's Law

= 560 mV / 1.47 kΩ

I_E = 0.381 mA

$I_C \approx I_E$

$I_C \approx 0.381$ mA

$P_{max} = I_C * V_C = I_C * V_0 = 0.381$ mA $* 3.52$ V_{peak}

$P_{max} = 1.34$ mW

$(V_E)^2 / R_E \leq P_{max}$

P_{max} $\geq (V_E)^2 / R_E$

$\geq (560$ mV$)^2 / 1.47$ kΩ

1.34 mW > 0.213 mW

The power dissipation in R_E is acceptable.

$V_{CE} * I_C \leq P_{max}$

P_{max} $\geq V_{CE} * I_C$

$\geq (3.52$ $V_{peak} - 560$ mV$) * 0.381$ mA

1.34 mW > 1.13 mW

The power dissipation in the BJT is acceptable.

$(V_{CC} - V_B)^2 / R_1 \leq P_{max}$

P_{max} $\geq (V_{CC} - V_B)^2 / R_1$

$\geq (10.00$ $V_{peak} - 2.56$ $V_{peak})^2 / 4.60$ kΩ

1.34 mW < 12.03 mW

According to the constraint, this specification regarding R_1's power dissipation is not met.

$(V_B)^2 / R_2 \leq P_{max}$

$P_{max} \geq (V_B)^2 / R_2$

$\geq (2.56 \text{ V})^2 / 6.67 \text{ k}\Omega$

1.34 mW > 0.983 mW

The power dissipation in R_2 is acceptable.

$I_{ch} = V_{CC} / (R_1 + R_2)$

$= 10 \text{ V} / (4.60 \text{ k}\Omega + 6.77 \text{ k}\Omega)$

$= 10 \text{ V} / (11.37 \text{ k}\Omega)$

$I_{ch} = 0.88 \text{ mA}$

$I_B = I_C / \beta$

$= 0.381 \text{ mA} / 500$

$I_B = 0.76 \text{ μA}$

Hence, $I_B \ll I_{ch}$

C.3 Verifying small-signal AC constraints

$g_m \approx I_C / V_T$

$\therefore \quad g_m \approx 0.381 \text{ mA} / 25 \text{ mV}$

$g_m \approx 15.2 \text{ }\Omega^{-1}$

$r_\pi = V_T / I_B = \beta / g_m = 500 / 15.2 \text{ }\Omega^{-1}$

$r_\pi = 32.9 \text{ }\Omega$

$R = (1/r_\pi + 1/R_2)^{-1} = R_2 * r_\pi / (R_2 + r_\pi)$

$= 6.77 \text{ k}\Omega * 32.9 \text{ }\Omega / (6.77 \text{ k}\Omega + 32.9 \text{ }\Omega)$

$R = 32.7 \text{ }\Omega$

$C_2 / C_1 = 81 \text{ pF} / 66 \text{ pF} = 1.23$

$g_m * R = 15.2 \text{ }\Omega^{-1} * 32.7 \text{ }\Omega = 497.0 \gg 1.23$

Therefore, $g_m * R \gg C_2 / C_1$ and the oscillator will oscillate as a result.

As aforementioned in 2.2.1, the output frequency is 20.06 MHz, which is within the range of acceptable values.

$\omega_0 = 2 * \pi * f_0 = 2 * \pi * 20.06 \text{ MHz} = 126.04 \text{ M rads}^{-1}$

$L_{B1} * \omega_0 > 30/(\omega_0 * C_2)$

0.97 mH * 126.04 M rads^{-1} > 30 / (126.04 M rads^{-1} * 81 pF)

122259 Hrads^{-1} > 2938.5 Fsrad^{-1}

$L_{B1} * \omega_0 > 30 * r_\pi$

122259 Hrads^{-1} > 30 * 15.2 Ω^{-1}

122259 Hrads^{-1} > 456 Ω^{-1}

$L_{B1} * \omega_0 > 30 * R_2$

122259 Hrads^{-1} > 30 * 6.67 kΩ

122259 Hrads^{-1} < 200100 Ω

$R_1 > 30 / (C_{B1} * \omega_0)$

4.60 kΩ > 30 / (1.020 µF * 126.04 M rads^{-1})

4.60 kΩ > 3856.82 Frads^{-1}

Hence, C_{B1} does connect nodes TP_1 and TP_2.

$R_E > 30 / (C_{B1} * \omega_0)$

1.47 kΩ > 30 / (679 pF * 126.04 M rads^{-1})

1.47 kΩ > 350.54 Frads^{-1}

Hence, C_{B2} does ground the emitter of the BJT

Appendix D Calculation and error analysis of L

D.1 Calculate the value of L

The measurements of C_1 and C_2 are:

$C_1 = (81 \pm 1)$ pF

$C_1 = (66 \pm 1)$ pF

$C \quad = (1/C_1 + 1/C_2)^{-1} = C_2 * C_1 / (C_2 + C_1)$

$\quad\quad = 66$ pF $* 81$ pF $/ (66$ pF $+ 81$ pF$)$

$C \quad = 36.37$ pF

$\omega_0 \quad = 1/\sqrt{(L*C)}$

$(\omega_0)^2 = 1/(L*C)$

$L \quad = 1/((\omega_0)^2 * C)$

$\quad\quad = (1/((126.04 \text{ M rads}^{-1})^2 * 36.37 \text{ pF}))$ H,

where $\omega_0 = 126.04$ M rads^{-1} as calculated in Appendix C.3

$L = 1.73$ µH

D.2 Calculate the absolute error of L

$C \quad = (1/C_1 + 1/C_2)^{-1} = C_2 * C_1 / (C_2 + C_1)$

Differentiate the expression for C and use the first order Taylor Series approximation to obtain the absolute error (Davis, BR 1997).

$\delta C = \partial C/\partial C_2 * \delta C_2 + \partial C/\partial C_1 * \delta C_1$

$\quad\quad = (C_2/ (C_2 + C_1) - C_2 * C_1 / (C_2 + C_1)^2) * \delta C_1 + (C_1 / (C_2 + C_1) - C_2 * C_1 / (C_2 + C_1)^2) * \delta C_2$

$\Delta C = (C_2/ (C_2 + C_1) - C_2 * C_1 / (C_2 + C_1)^2) * \Delta C_1 +$

$\quad\quad (C_1 / (C_2 + C_1) - C_2 * C_1 / (C_2 + C_1)^2) * \Delta C_2$

$\quad\quad = (81 \text{ pF}/(81 \text{ pF} + 66 \text{ pF}) - 81 \text{ pF} * 66 \text{ pF}/(81 \text{ pF} + 66 \text{ pF})^2) * 1 \text{ pF} +$

$\quad\quad (66 \text{ pF}/(81 \text{ pF} + 66 \text{ pF}) - 81 \text{ pF} * 66 \text{ pF}/(81 \text{ pF} + 66 \text{ pF})^2) * 1 \text{ pF}$

$\quad\quad = (0.551 - 0.247) * 1 \text{ pF} + (0.449 - 0.247) * 1 \text{ pF}$

$\quad\quad = 0.304 \text{ pF} + 0.202 \text{ pF}$

$\quad\quad = 0.506 \text{ pF}$

$\omega_0 = 2*\pi*f_0$

$\Delta\omega_0 / \omega_0 = \Delta f_0 / f_0$

$\Delta\omega_0 = \Delta f_0 / f_0 * \omega_0$

$= (0.01 \text{ MHz} / 20.06 \text{ MHz}) * 126.04 \text{ M rads}^{-1}$

$= 0.06 \text{ Mrads}^{-1}$

$L \quad = 1/((\omega_0)^2 * C)$

$\Delta L / L = 2 * \Delta\omega_0 / \omega_0 + \Delta C / C$

$\Delta L = (2 * \Delta\omega_0 / \omega_0 + \Delta C / C) * L$

$\quad\quad = (2 * 0.06 / 126.04 + 0.506 / 36.37) * 1.73 \text{ μH}$

$\Delta L = 0.02 \text{ μH}$

Hence, the absolute error of L is 0.02 μH.

The calculated value of L is (1.73 ± 0.02) μH.

Appendix E   Calculation of %THD for different points of the circuit.

E.1   Calculate the %THD at TP$_3$

%THD at TP$_3$ $= \sqrt{(47^2 + 38^2 + 30^2 + 22^2 + 19^2 + 18^2)} / 61 * 100\%$

$= 1.24\%$

E.2   Calculate the %THD at TP$_2$

%THD at TP$_3$ $= \sqrt{(51^2 + 40^2 + 36^2 + 22^2 + 22^2 + 20^2)} / 64 * 100\%$

$= 1.29\%$

E.3   Calculate the %THD at the emitter of the BJT

%THD at TP$_3$ $= \sqrt{(50^2 + 45^2 + 38^2 + 34^2 + 34^2 + 19^2)} / 62 * 100\%$

$= 1.50\%$

Appendix F Calculations of the values of circuit components for the emitter follower

F.1 Calculations for circuit components values of the buffer

Choose the load resistor, R_L, to be 1.0 kΩ, V_{CC} = 10 V and V_{BE} = 0.6 V as aforementioned.

As aforementioned, I_C is approximately equal to I_E. As shown in Figure 6, the maximum value of β lies between 0.1 mA and 10 mA for value of I_C. Since I_E is dependent on the current required at the input of the load, I_E is chosen to be 3 mA.

Choose V_{CE} = 0.4 * V_{CC}

Hence, V_{CE} = 0.4 * 10 V = 4 V

Thus, $V_E = V_{CC} - V_{CE}$ = 10 V − 4 V = 6 V

$R_E = V_E / I_E$ = 6 V / 3 mA = 2.0 kΩ, by Ohm's Law

Change R_E to 2.2 kΩ since there are no 2 kΩ resistors in the laboratories.

Applying the voltage divider principle yields,
$$R_2 / (R_1 + R_2) = (V_{BE} + V_E) / V_{CC} = V_B / V_{CC}$$

$R_2 / (R_1 + R_2)$ = (0.6 V + 6 V) / 10 V = 0.66

R_2 = 0.66 * ($R_1 + R_2$)

0.66 * R_1 = 0.34 * R_2

R_1 = 0.34 / 0.66 R_2 = 0.51 * R_2

To apply the voltage divider principle, the chain current of the emitter follower, I_{ch}, must be much larger than that of the base current.
$$I_{ch} \gg I_B \text{ becomes } I_{ch} > 30 * I_B$$

Since $I_B = I_C / \beta = I_C / 500$, where β = 500 as aforementioned in Section 2.1.4, let $I_{ch} = I_E / 10$.

Thus, $I_{ch} = I_E / 10$ = 3 mA / 10 = 0.3 mA

Since $I_{ch} = V_{CC} / (R_1 + R_2)$ as aforementioned in Section 2.1.4,

I_{ch} = 0.3 mA = $V_{CC} / (R_1 + R_2)$ = 10 V / (0.51 * $R_2 + R_2$)

$\therefore$ R_2 = 22.0 kΩ & R_1 = 11.3 kΩ.

Select R_1 to be 10 kΩ since there are no 11.3 kΩ resistors in the laboratories.

$Z = R + X_C + X_L = X_C$, since X_L and $R = 0$ (Franco, S 1995)

$X_C = 1 / (j\omega * C)$

∴ $X_C = 1/ (\omega * C)$, ignoring the complex domain.

Choose C_1 to be sufficiently large so that it acts as a short circuit at high frequencies of 20 MHz. This implies that X_C must be as small as possible. Hence, let $X_C = 1$.

∴ $C_1 \geq 1 / \omega$

$C_1 \geq 1 / 125.66$ Mrads^{-1}

$C_1 \geq 8$ nF

Choose C_1 to be 1 μF. Similarly, choose $C_2 = C_1 = 1$μF.